Carbohydrate nanotubes production and its techno-economic validation

Bioresource Technology Reports

Carbohydrate Nano-tubes Production and its Techno-economic Validation

--Manuscript Draft--

Manuscript Number:	BITEB-D-22-01222R3
Article Type:	Original research paper
Keywords:	Corncob; cellulose; Trichoderma reesei; Cellulase; hydrolysis; Carbohydrate nanotubes
Corresponding Author:	Athanasios A. Koutinas Patra, GREECE
First Author:	Athanasia Panitsa
Order of Authors:	Athanasia Panitsa
	Theano Petsi
	Eleana Kordouli
	Poonam Singh Nigam
	Maria Kanellaki
	Athanasios A. Koutinas
Abstract:	The production of carbohydrate nanotubes (CHNTs) using agricultural wastes is proposed in this investigation. The corncob was found to be the most productive for our purpose among the four lignocellulosic raw materials tested. CHNTs production was accomplished in two stages. Tubular cellulose (TC) was prepared from raw substrates through a delignification process, and the prepared tubes of TC were cut into nano-size carbohydrate tubes in a chemical-free process. To achieve this, cellulase was produced in our lab using agricultural residue, employing the non-pathogenic fungus Trichoderma reesei, a high cellulase producer. Analysis of the produced CHNTs proved stability, nano-dimension lengths, and increased crystallinity. The technoeconomic feasibility report showed that the production of CHNTs is cost-effective. This was supported by a process flow sheet with mass and energy balances based on laboratory experimental results.

Graphical Abstract (for New review)

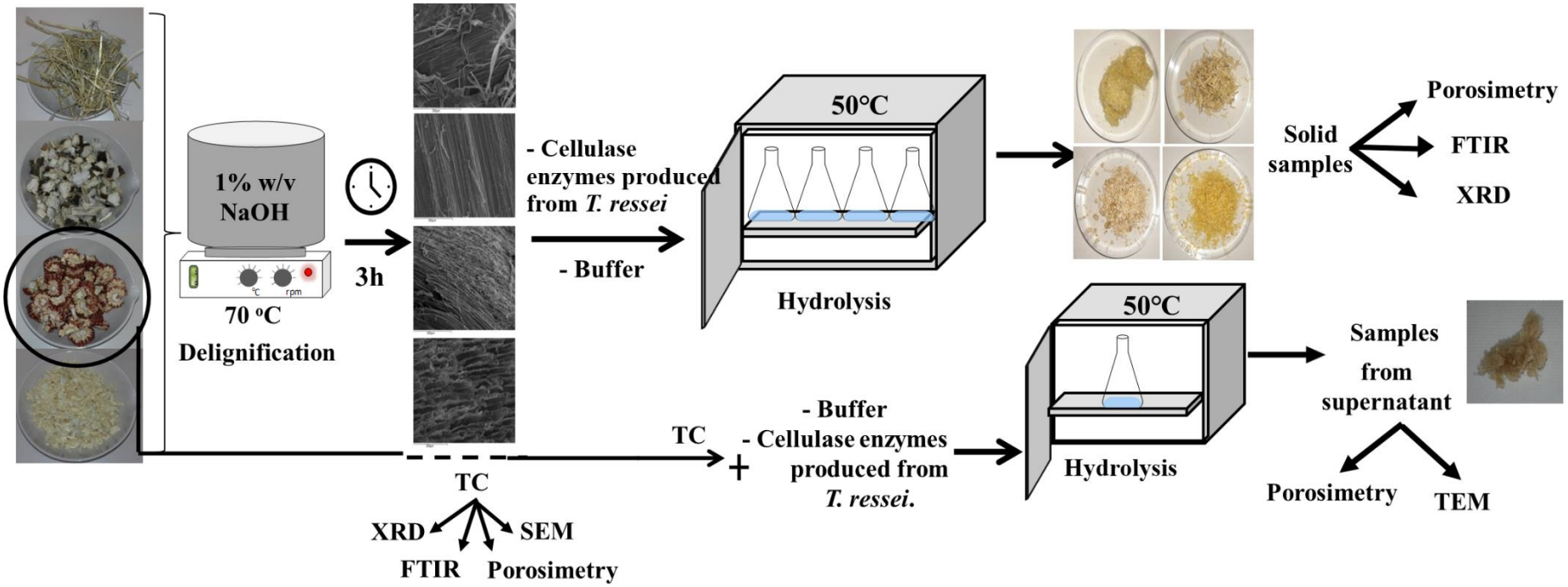

Highlights

- Corncob treatment provide a cellulosic material with nanotubes
- The surface characteristics of corncob favored the formation of nanotubes
- CHNts were present in the supernatant of the hydrolysis suspension
- Technoeconomic-feasibility report validated a cost-effective CHNTs production

Carbohydrate Nanotubes Production and its Techno-economic Validation

Athanasia Panitsa[a], Theano Petsi[a], Eleana Kordouli[a], Poonam Singh Nigam[b], Maria Kanellaki[a], Athanasios A. Koutinas[a*]

[a] Food Biotechnology Group, Department of Chemistry, University of Patras, Patras, Greece.

[b] Biomedical Sciences Research institute, Ulster University, Coleraine, N. Ireland, UK.

sissy_panitsa@hotmail.com, thpetsi@upatras.gr, ekordouli@upatras.gr, p.singh@ulster.ac.uk, M.Kanellaki@upatras.gr, A.A.Koutinas@upatras.gr

**Corresponding author*

Tel:0030.2610.997104 e-mail:A.A.Koutinas@upatras.gr

ABSTRACT

The production of carbohydrate nanotubes (CHNTs) using agricultural wastes is proposed in this investigation. The corncob was found to be the most productive for our purpose among the four lignocellulosic raw materials tested. CHNTs production was accomplished in two stages. Tubular cellulose (TC) was prepared from raw substrates through a delignification process, and the prepared tubes of TC were cut into nano-size carbohydrate tubes in a chemical-free process. To achieve this, cellulase was produced in our lab using agricultural residue, employing the non-pathogenic fungus *Trichoderma reesei*, a high cellulase producer. Analysis of the produced CHNTs proved stability, nano-dimension lengths, and increased crystallinity. The technoeconomic feasibility report showed that the production of CHNTs is cost-effective. This was supported by a process flow sheet with mass and energy balances based on laboratory experimental results.

KEYWORDS: *corncob; cellulose; Trichoderma reesei; cellulase; hydrolysis; Carbohydrate nanotubes*.

1. Introduction

Over the past few decades, nanotechnology, nano-synthetic materials, and their applications have gained attention. Carbon nanotubes (CNTs) are among the most commonly used nanomaterials. These CNTs are rolled graphene with sp^2 hybridization and can be divided into three categories, according to the number of tubes present in CNTs: single-walled CNTs, double-walled CNTs, and multi-walled CNTs (Eatemadi et al., 2014; Ibrahim, 2013). Information on CNTs was first published in 1991 (Lijima, 1991), and since then this nanomaterial has established rapidly growing applications in sensors, nanomedicine, environment, energy, and others (Ibrahim, 2013). However, their use in the biological and biomedical sectors of the human system is restricted due to their increased toxicity to the human body. The size of nanotubes can affect the toxicity of CNTs, particularly those with a size under 100 nm. They can affect the lungs and whole respiratory system by activating immunological responses modifying protein structure, and these re-disperse from their site of deposition in the human system (Eatemadi et al., 2014; Satishkumar et al., 2000). Prolonged and excessive exposure to CNTs can cause inflammation and oxidative stress (Nemmar et al., 2001).

In order to avoid the side effects of CNT use, we anticipated that alternative agricultural materials could be used for nanotubes production. Inexpensive and renewable natural resources were explored for the production of carbohydrate nanotubes (CHNTs). Such materials can be made from residual plant stalks, which are generated as by-products of each crop. Globally, enormous amounts of agricultural waste, such as wheat straw, sunflower stems, and corncobs, are produced each year following the harvesting of wheat grains, corn, and sunflower seeds. (Barouni et al., 2015; Bian et al., 2018; Cavali et al., 2020; Chen et al., 2021; FAO, 2019; Koutinas et al., 2016a; USDA, 2021). Nanofibers produced from natural cellulosic waste materials and their application in nanocomposite materials are topics in Green Advance. The advantages of cellulose nanofibers include their biodegradability, biocompatibility, renewable nature, high strength and stiffness, and low weight. (Kumar et al., 2020; Reddy and Rhim, 2014; Sosiati et al., 2014). Furthermore, nanocellulose's structure can be modified to meet the needs of particular applications by not only using a particular agricultural product as the material's initial carbon source but also by improving or changing the method of production. Nanocelluloses have

proven to be possible fillers for the improvement of the mechanical properties of biopolymer films, such as starch, alginate, and chitosan films (Barouni et al., 2015; Koutinas et al., 2016a; Kumar et al., 2020; Reddy and Rhim, 2014; Shankar and Rhim, 2016). Our previous studies have shown that lignocellulosic material after delignification can be used for the formation of tubular cellulose with micro and nano dimensions (Koutinas et al., 2016b). The aim of this work was the production of carbohydrate nanotubes (CHNTs), a new generation of nanotubes, from the carbon content of agricultural residues via the preparation of tubular cellulose (TC) in an enzymatic process.

2. Experimental

2.1 Agricultural residual materials

In our experiments, we used free or low-cost materials such as corncob and sunflower stems from local farms, wheat straw from a local cattle feed market, and sawdust from a local timber mill.

2.2 Cellulase preparation

For a green, economical technology, we used cellulolytic enzymes prepared in our lab from carbon sources of agricultural origin. A high cellulase-producer, *Trichoderma reesei* (ATCC 26921), was grown on Potato Dextrose Agar (PDA) medium at 30 °C for 5-7 days. Fungal spores were aseptically collected from the surface of PDA plates by gently scraping with sterilized water and were counted on a hemocytometer (Neubauer Improved, HBG, Germany). The production of cellulase was carried out using a modified method by Li et al. (2013). Two mL of spore suspension containing 10^6-10^7 spores mL^{-1} was precultured in 60 mL of sterilized medium consisting of 2% w/v delignified sawdust, 1% soy peptone, and 1% glucose. The pH of the medium was adjusted to 4.5 with a 2M NaOH solution and incubated in a VELP Scientifica FOC incubator at 30 °C and 180 rpm for 24 h. Forty mL of freshly grown preculture was aseptically added into a 2 L bioreactor (Electrolab), containing 1 L of sterilized medium made of 25 g delignified sawdust, 1.7% soy peptone, 0.5% $(NH_4)_2SO_4$, 0.6% KH_2PO_4, 0.2% $MgSO_4 \cdot 7H_2O$, 0.25% glycerol, and 2 mL Tween 20. The bioreactor equipped with the control devices Fermac 231/260 was operated at 26 °C, 300 rpm, 1.5 L/min ventilation and pH 4.5–5.0. After 150 h of

fungal growth, the content was aseptically centrifuged to obtain a clear supernatant for use as a crude preparation of cellulolytic enzyme.

2.3 Assay of cellulase activity

One mL of crude enzyme (prepared as above) was mixed with 100 mL of sodium citrate buffer (pH 5.0). From this, 5 mL was placed in a 50 mL conical flask with 10 mL of buffer and 0.5 g of finely stripped Whatman filter paper. The reaction mixture was incubated at 50 °C for 60 min, and the released glucose due to enzyme activity was measured by High Performance Liquid Chromatography (HPLC) on a Shimadzu LC-9A. Enzyme units were calculated against a standard curve plotted for glucose released in a similar reaction conducted with a commercial cellulase with known units (Chu et al., 2012).

2.4 Stage-1 Preparation of tubular cellulose (TC)

Lignocellulosic materials, including corncob, sunflower stem, wheat straw, and sawdust, were subjected to a very mild (1%, w/v) NaOH solution treatment for three hours at 70 °C. Materials were filtered out and washed with hot (90 □ -95 □) deionized water for complete removal of NaOH and released lignin. The delignified material produced in this procedure was employed as TC in a later stage; therefore, it was freeze-dried at 15×10^{-3} mbar and -45 °C using a Labtech Daihan Freeze Dry System.

2.5 Stage-2 Enzymatic treatment of TC to develop CHNTs

In separate flasks containing 200 mL of buffer pH 5.0 and 10 mL of crude enzyme, 15 g of TC prepared from four agricultural residues were incubated at 50 °C for 72 hours without stirring or mixing. To examine the formation of CHNTs samples from the flasks of each substrate were taken at 5, 24, 48, and 72 h intervals.

2.6 Stage-3 Isolation of CHNTs

After hydrolysis of TC a quantity of clear supernatant liquid without dispersed solids was taken in order to isolate the water-soluble CHNTs. The liquid was freeze-dried, and porosimetry and TEM analysis were performed in the powder received.

105 2.7 Examination of CHNTs

106 Following all Standard Operating Procedures (SOPs) for each equipment used, examination of CHNTs
107 was conducted as below: Specific surface area, pore size distribution, and pore volume of all types of
108 materials (original raw material, TC, and CHNT) was carried out by N_2 adsorption-desorption process
109 at -196.15 °C on a Tristar 3000 porosimeter (Micromeritics); Jeol Model JSM-5600LV scanning elec-
110 tron microscope was used operating at an accelerating voltage of 20 kV; X-ray powder diffractometry
111 (XRD) was used to test the crystallinity of materials on a Bruker AXS D8 ADVANCE at 40 kV and 20
112 mA. Segal's equation based on the diffraction pattern intensity was used for the calculation of the
113 crystallinity index (CI). Transmission Electron Microscopy (TEM) images were taken with the help of
114 a Gatan model 782 Erlangshen E5500W camera. FTIR spectra of samples were obtained using a FTIR
115 Perkin-Elmer spectrophotometer, 16 PC model, in the range of 4000–400 cm^{-1}.

116 2.8 Technoeconomic validation and Process Flow Sheet for industrial application

117 Details of the process flow sheet design are presented in Figure 5, and the investment and daily pro-
118 duction costs are presented in Tables 4 and 5, respectively. The delignification of biomass takes place
119 in tank 1, by supplying steam through a boiler (11) and the delignified cellulosic material is transferred
120 to enzyme production bioreactor (2) and CHNT production bioreactor (5). The enzyme production bio-
121 reactor (2) is supplied with air by an air pump (4) through a sterile filter (3). The temperature in biore-
122 actors 2 and 5 is kept constant at 26 □ and 50 □ respectively, by supplying steam from the boiler (11).
123 The hydrolysate from the bioreactor 5 containing CHNTs is pumped to the centrifugal separator (7) to
124 separate suspended solids from the solution of CHNTs. A clear CHNTs solution is collected in tank 8,
125 then concentrated in a condenser (9), and subsequently freeze-dried in a freeze-dryer system (10).

126

127 3. Results and Discussion

128 3.1 Structure of TC

From the SEM images (Fig. S1) of wheat straw, sunflower stem, corncob, and sawdust (original and delignified), it can be observed that the morphology of the materials changed after delignification, pores were created on the surface of the materials, and the fibers arranged in TC could be seen (Fig. S1)These changes are attributed to the removal of amorphous areas, which was earlier occupied by lignin and hemicellulose contents in raw substrates (Cavali et al., 2020). The two naturally occurring forms of cellulose are Iα and Iβ. In this analysis, only Iβ was visible, as it is part of higher plants, in contrast to the form Iα only found in bacterial and algae celluloses (Poletto et al., 2014). Studies of atomic resolution synchrotron and neutron diffraction data, have shown that cellulose Iα has a triclinic unit cell P1 ($a = 6.717$ Å, $b = 5.9962$ Å, $c = 10.400$ Å, $\alpha = 118.08°$, $\beta = 114.80°$, and $\gamma = 80.37°$) containing a single cellulose chain, while cellulose Iβ has a monoclinic unit cell P21 ($a = 7.784$ Å, $b = 8.201$ Å, $c = 10.380$ Å, $\alpha = \beta = 90°$, $\gamma = 96.5°$) containing two conformationally distinct cellulose chains, called original chains and central chain (Krichen et al., 2022). The structure of cellulose Iβ is mainly in the form of parallel chains linked by H-bonds stacked with an alternating shear parallel to the chain axis stabilized by Van der Waals interactions (Poletto et al., 2014). After delignification of materials, the specific surface area of TC (Table 1) was about 2-fold higher due to the formation of cellulose tubes in the space created by the removal of lignin fraction. The pore volume and pore size were also increased, except for TC prepared from sunflower stem, which had a lower specific surface area (Table 1).

3.2 Crystallinity analysis

The degree of cellulose crystallinity plays an important role in cellulose structure parameters. Since the crystal structure of cellulose affects the enzymatic hydrolysis (Park et al., 2010), the crystallinity was examined in XRD analysis (Fig. 1 and Table 2). The characteristic peaks of Iβ cellulose were observed at 2θ (theta) of about 16º, and 22.64º (Banvillet et al., 2021; Bian et al., 2018; Ling et al., 2021; Zhang et al., 2021). The sharper peaks in the XRD profile of TC materials indicate that their degree of crystallinity was higher compared to that of the raw materials. For delignified sawdust, sunflower stem, and wheat straw, a peak located at 2θ of about 30.0° was also identified. This can be an indication of amorphous areas after delignification (Sosiati et al., 2015; Sosiati and Harsojo, 2014). Another

characteristic peak of cellulose Iβ at 2θ of about 35.0° appeared for all materials (Banvillet et al., 2021; Ling et al., 2021; Zhang et al., 2021). An increase in the rigidity of cellulose tubes (fibers) and a decrease in their flexibility occur when there is an increase in the ratio of crystalline to amorphous regions. Sunflower stem and corn cob had the lowest crystallinity indices (CI) (Table 2). CI increases as the surface area of the crystallites corresponds to decrease in amorphous cellulose, due to the void spaces available after lignin removal (Cavali et al., 2020; Poletto et al., 2014).

3.3 FT-IR spectra

The spectra for corncob and wheat-straw are presented in Figs. 2a and 2b, for the other two materials, spectra were similar (hence not presented here). At around 3440-3420 cm^{-1} an intramolecular H-bond vibration appeared, which indicates cellulose (Poletto et al., 2014). The FTIR absorption peaks at ~2900 cm^{-1} are characteristic of the stretching vibration of C-H groups of cellulose (Reddy and Rhim, 2014). The absorption peaks at 1440-1430 cm^{-1} are due to CH_2 bending vibration and indicate the "crystallinity band" in the cellulose. A reduction or expansion in the intensity of this crystallinity band among the untreated, delignified freeze dried, and after enzymatic hydrolysis samples indicates that the level of crystallinity of cellulose crystals decreased/increased during treatment processes (Shankar and Rhim, 2016). The peaks appeared at 1375 cm^{-1} are typical of the O-H bending vibration of cellulose. The peaks at 1163-1165 cm^{-1} are attributed to the C-O-C pyranose ring stretching vibration and the peaks at 896-898 cm^{-1} indicate the C-H rocking vibration of cellulose present in the microfibers and nanofibers (Reddy and Rhim, 2014). No considerable changes in the absorption peak positions of untreated and delignified freeze-dried samples (TC), were observed (Figs. 2a and 2b), which indicated that these processes did not alter the chemical structure of the cellulosic materials. However, the spectra bands present at around 1730 cm^{-1} in raw lignocellulosic (due to C-O stretching vibration for the acetyl and ester linkages in lignin/hemicellulose) were absent in the spectra of TC. That confirmed the absence of lignin and hemicellulose in TC, which were removed in stage 1 of alkali treatment (Gabriel et al., 2020; Kargarzadeh et al., 2012; Kumar et al., 2020).

3.4 Enzyme treatment of TC for development of CHNTs

TC materials were treated with our lab-prepared crude cellulase (70 FPU/g) to develop CHNTs. N_2 adsortion-desorption porosimetry analysis (Figs. 3a, b, c) show the kinetics: BET surface area (m^2/g) and pore volume are given by BJH equation, and the pore size by BET (nm). CHNTs were produced after 24 h enzyme treatment of TC obtained from four agricultural substrates. CHNTs from corn cob presented the highest value of surface area (1.8 m^2/g), which is a desired parameter for the entrapment of pharmaceutical substances, food preservatives, and other entities in CHNTs (Panitsa et al., 2021). Based on the number of tubes with pore widths between 2-70 nm (Fig. 3d) in combination with pore volume (0.013 cm^3/g) and the average pore diameter (13.5 nm), corncob-TC proved to be the most productive material among the TC of other substrates, for the development of CHNTs.

3.5 Physicochemical properties of the isolated CHNTs product

CHNTs retain some important properties of cellulose, such as biodegradability and non-toxicity. CHNTs are oligomers with glucose as their structural unit and can form hydrogen bonds with OH groups containing enzymes and drugs. The characterization of the isolated product of CHNTs was carried out by TEM to prove the nanodimensions of the length of tubes. Porosimetry analysis confirmed the pore size (Table 3) and pore distribution (Fig. S3), classifying the material, a nanomaterial.

3.5.1 Transmission Electron Microscopy of the isolated CHNTs product

TEM images of CHNTs developed from corncob showed needle-like cellulosic nanotubes (Fig. 4 a, b) with an internal diameter 6-16 nm and a length of tubes in the range of 80-160 nm. These data proved that the cellulosic tubes in TC after treatment with cellulolytic enzymes produced carbohydrate nanotubes (CHNTs).

3.5.2 Porosimetry analysis of the isolated CHNTs product

The BET surface area was 1.35 m^2/g and the pore width was 4.6 nm after 72 hours of hydrolysis, as shown in Table 3. Porosimetry measurement revealed an average pore diameter (tube diameter) of around 4-5 nm (Fig. 4b), which is consistent with the size of the tubes depicted in the TEM image.

3.6 Design and operation of the bioreactor and economic validation of technology

The bioreactor system presented in Figure 5 contains bioreactor 2 of 10,000 L for enzyme production and bioreactor 5 of 100,000 L for tubular cellulose (TC) hydrolysis to nanotubes. Machineries of high cost are the condenser (9), freeze dryer (10), and centrifugal separator (7). The boiler (11) that produces 850 liters of oil per day and the delignification tank (1) are also of importance. Delignification tanks (1) and condensers (9), respectively, need about 87% of steam consumption. Centrifugal separators (7) and freeze dryers (10) need more than 90% electricity consumption. The total investment cost has been calculated at €1,743,000, with the biggest costs being those of the condenser (€300,000), freeze dryer (€500,000), and boiler (€600,000). The parameters considered for the calculation of the daily production cost were raw material cost, labor, thermal energy, electricity, water requirement, consumables, and investment payment costs. The biggest costs are the labor cost and that of thermal energy, which are about 70% of the €2,731 daily cost. On the other hand, the annual turnover is equal to about €1,500,000, which could give a profit of €300,000 annually. So, it is estimated that the payment of investment costs will be achieved in about 6 years. This short period of investment repayment shows that the technology has a large margin of profit to convince the investors to proceed.

3.7. Technological and scientific implications

The aforementioned presentation of results and discussion have demonstrated the production of CHNTs. Specifically, the XRD and FTIR analysis proved that the tubes consist of cellulose,

229 while lignin and hemicelluloses have been removed. They also proved the increment of crys-
230 tallinity indices, which is related to the rigidity of tubes. The formation of a new generation of
231 tubes could lead to the preparation of a carrier material potentially usable as a drug delivery
232 system. The metabolism and safety of CHNTs in the human body should be examined. Immo-
233 bilization of cellulase in CHNT tubes with pharmaceutical substances could be considered a
234 possible method for removing the carrier material from the body after its action. Cellulase has
235 the ability to hydrolyze cellulose into glucose, a nutrient for humans. Finally, the method of
236 producing CHNTs is feasible, and the raw material is sustainable. The technoeconomic valida-
237 tion based on laboratory results showed that the process is cost-effective. This is supported by
238 laboratory results (Table S1).

239

240 **4. Conclusions**

241 The Technoeconomic feasibility report validated that CHNT production is cost-effective. A green tech-
242 nology was applied for four agricultural residual materials. Among them, corncob has proved the most
243 productive. It is free, making our process economically viable. TC tubes from corncob were cut short
244 with cellulase, a cheaper lab preparation from *Trichoderma reesei*, to carbohydrate tubes of nano-size.
245 FTIR and XRD analysis revealed the stability of CHNT's chemical structure. CHNTs were isolated
246 from the solution of hydrolyzed cellulose after freeze-drying. The nano-dimension tubes of the final
247 product were confirmed by TEM and porosimetry analysis. CHNTs-based carrier materials could po-
248 tentially be used as drug delivery systems. However, their metabolism in the human body should be
249 studied for their safety.

250

251 E-supplementary data for this work can be found in e-version of this paper online

252 .

Acknowledgements

We acknowledge support of this work by the project "Research Infrastructure on Food Bioprocessing Development and Innovation Exploitation – Food Innovation RI" (MIS 5027222), which is implemented under the Action "Reinforcement of the Research and Innovation Infrastructure", funded by the Operational Programme "Competitiveness, Entrepreneurship and Innovation" (NSRF 2014–2020) and co-financed by Greece and the European Union (European Regional Development Fund).

Funding

This work was supported by the project "Research Infrastructure on Food Bioprocessing Development and Innovation Exploitation – Food Innovation RI" (MIS 5027222), which is implemented under the Action "Reinforcement of the Research and Innovation Infrastructure", funded by the Operational Programme "Competitiveness, Entrepreneurship and Innovation" (NSRF 2014–2020) and co-financed by Greece and the European Union (European Regional Development Fund).

Declaration of interest: none.

The authors declare that they have no known competing financial interests or personal relationships that could have appeared to influence the work reported in this paper.

CRediT authorship contribution statement

All authors contributed to the study conception and design. **Athanasia Panitsa**: Methodology, Validation, Investigation, original draft, Visualization. **Theano Petsi**: Methodology, Writing-review & editing. **Eleana Kordouli:** Methodology, Validation. **Poonam S. Nigam**: Result-analysis for writing-second draft, editing. **Maria Kanellaki**: Supervision. **Athanasios A. Koutinas**: Conceptualization, Writing-original draft, Project-administration, Funding-acquisition. All authors read and approved the final manuscript.

276

REFERENCES

1. Banvillet, G., Gatt, E., Belgacem, N., Bras, J., 2021. Cellulose fibers deconstruction by twin-screw extrusion with in situ enzymatic hydrolysis via bioextrusion. Bioresour. Technol. 327, 124819. https://doi.org/10.1016/j.biortech.2021.124819

2. Barouni, E., Petsi, T., Kanellaki, M., Bekatorou, A., Koutinas, A., 2015. Tubular cellulose/starch gel composite as food enzyme storehouse. Food Chem. 188, 106–110. https://doi.org/10.1016/j.foodchem.2015.04.038

3. Bian, H., Gao, Y., Yang, Y., Fang, G., Dai, H., 2018. Improving cellulose nanofibrillation of waste wheat straw using the combined methods of prewashing, p-toluenesulfonic acid hydrolysis, disk grinding, and endoglucanase post-treatment. Bioresour. Technol. 256, 321–327. https://doi.org/10.1016/j.biortech.2018.02.038

4. Cavali, M., Soccol, C.R., Tavares, D., Zevallos Torres, L.A., Oliveira de Andrade Tanobe, V., Zandoná Filho, A., Woiciechowski, A.L., 2020. Effect of sequential acid-alkaline treatment on physical and chemical characteristics of lignin and cellulose from pine (Pinus spp.) residual sawdust. Bioresour. Technol. 316, 123884. https://doi.org/10.1016/j.biortech.2020.123884

5. Chen, H., Mao, J., Jiang, B., Wu, W., Jin, Y., 2021. Carbonate-oxygen pretreatment of waste wheat straw for enhancing enzymatic saccharification. Process Biochem. 104, 117–123. https://doi.org/10.1016/j.procbio.2021.03.016

6. Chu, D., Deng, H., Zhang, X., Zhang, J., Bao, J., 2012. A simplified filter paper assay method of cellulase enzymes based on HPLC analysis. Appl. Biochem. Biotechnol. 167, 190–196. https://doi.org/10.1007/s12010-012-9673-0

7. Eatemadi, A., Daraee, H., Karimkhanloo, H., Kouhi, M., Zarghami, N., Akbarzadeh, A.,

300 Abasi, M., Hanifehpour, Y., Joo, S.W., 2014. Carbon nanotubes: Properties, synthesis,
301 purification, and medical applications. Nanoscale Res. Lett. 9,393.
302 https://doi.org/10.1186/1556-276X-9-393

303 8. FAO, 2019. Forest Products Annual Market Review, 2018-2019, Unece.

304 9. Gabriel, T., Belete, A., Syrowatka, F., Neubert, R.H.H., Gebre-Mariam, T., 2020.
305 Extraction and characterization of celluloses from various plant byproducts. Int. J. Biol.
306 Macromol. 158, 1248–1258. https://doi.org/10.1016/j.ijbiomac.2020.04.264

307 10. Ibrahim, K.S., 2013. Carbon nanotubes-properties and applications: a review. Carbon
308 Lett. 14, 131–144. https://doi.org/10.5714/cl.2013.14.3.131

309 11. Kargarzadeh, H., Ahmad, I., Abdullah, I., Dufresne, A., Zainudin, S.Y., Sheltami, R.M.,
310 2012. Effects of hydrolysis conditions on the morphology, crystallinity, and thermal stability
311 of cellulose nanocrystals extracted from kenaf bast fibers. Cellulose 19, 855–866.
312 https://doi.org/10.1007/s10570-012-9684-6

313 12. Koutinas, A., Papafotopoulou-Patrinou, E., Gialleli, A.I., Petsi, T., Bekatorou, A.,
314 Kanellaki, M., 2016a. Production of nanotubes in delignified porous cellulosic materials after
315 hydrolysis with cellulase. Bioresour. Technol. 213, 169–171.
316 https://doi.org/10.1016/j.biortech.2016.03.065

317 13. Koutinas, A., Papafotopoulou-Patrinou, E., Gialleli, A.I., Petsi, T., Bekatorou, A.,
318 Kanellaki, M., 2016b. Production of nanotubes in delignified porous cellulosic materials after
319 hydrolysis with cellulase. Bioresour. Technol. 213, 169–171.
320 https://doi.org/10.1016/j.biortech.2016.03.065

321 14. Krichen, F., Walha, S., Abdelmouleh, M., 2022. Hirshfeld surface analysis of the
322 intermolecular interaction networks in cellulose *Iα* and *Iβ*. Carbohydr. Res. 518, 108600.

https://doi.org/10.1016/j.carres.2022.108600

15. Kumar, A., Singh Negi, Y., Choudhary, V., Kant Bhardwaj, N., 2020. Characterization of Cellulose Nanocrystals Produced by Acid-Hydrolysis from Sugarcane Bagasse as Agro-Waste. J. Mater. Phys. Chem. 2, 1–8. https://doi.org/10.12691/jmpc-2-1-1

16. Li, C., Yang, Z., He Can Zhang, R., Zhang, D., Chen, S., Ma, L., 2013. Effect of pH on cellulase production and morphology of Trichoderma reesei and the application in cellulosic material hydrolysis. J. Biotechnol. 168, 470–477. https://doi.org/10.1016/j.jbiotec.2013.10.003

17. Lijima, S., 1991. Helical microtubules of graphitic carbon. Nature 354, 56-58. https://doi.org/10.1038/354056a0

18. Ling, Z., Tang, W., Su, Y., Shao, L., Wang, P., Ren, Y., Huang, C., 2021. Bioresource Technology Promoting enzymatic hydrolysis of aggregated bamboo crystalline cellulose by fast microwave-assisted dicarboxylic acid deep eutectic solvents pretreatments. Bioresour. Technol. 333, 125122. https://doi.org/10.1016/j.biortech.2021.125122

19. Nemmar, A., Vanbilloen, H., Hoylaerts, M.F., Hoet, P.H.M., Verbruggen, A., Nemery, B., 2001. Passage of Intratracheally Instilled Ultrafine Particles from the Lung into the Systemic Circulation in Hamster. Br. Commun. Am J Respir Crit Care Med 164, 1665–1668. https://doi.org/10.1164/rccm2101036

20. Panitsa, A., Petsi, T., Kandylis, P., Nigam, P.S., Kanellaki, M., Koutinas, A.A., 2021. Chemical preservative delivery in meat using edible vegetable tubular cellulose. LWT141, 111049. https://doi.org/10.1016/j.lwt.2021.111049

21. Park, S., Baker, J.O., Himmel, M.E., Parilla, P.A., Johnson, D.K., 2010. Cellulose crystallinity index: Measurement techniques and their impact on interpreting cellulase

346 performance. Biotechnol. Biofuels 3, 10. https://doi.org/10.1186/1754-6834-3-10

347 22. Poletto, M., Ornaghi Júnior, H.L., Zattera, A.J., 2014. Native cellulose: Structure,
348 characterization and thermal properties. Materials (Basel). 7, 6105–6119.
349 https://doi.org/10.3390/ma7096105

350 23. Reddy, J.P., Rhim, J.W., 2014. Characterization of bionanocomposite films prepared with
351 agar and paper-mulberry pulp nanocellulose. Carbohydr. Polym. 110, 480–488.
352 https://doi.org/10.1016/j.carbpol.2014.04.056

353 24. Satishkumar, B.C., Govindaraj, A., Nath, M., Rao, C.N.R., 2000. Synthesis of metal oxide
354 nanorods using carbon nanotubes as templates. J. Mater. Chem. 10, 2115–2119.
355 https://doi.org/10.1039/b002868l

356 25. Shankar, S., Rhim, J.W., 2016. Preparation of nanocellulose from micro-crystalline
357 cellulose: The effect on the performance and properties of agar-based composite films.
358 Carbohydr. Polym. 135, 18–26. https://doi.org/10.1016/j.carbpol.2015.08.082

359 26. Sosiati, H., Harsojo, H., 2014. Effect of combined treatment methods on the crystallinity
360 and surface morphology of kenaf bast fibers. Cellul. Chem. Technol. 48 (1), 33–43.

361 27. Sosiati, H., Muhaimin, M., Purwanto, Wijayanti, D.A., Harsojo, Soekrisno, Triyana, K.,
362 2015. Microscopic characterization of cellulose nanocrystals isolated from sisal fibers. Mater.
363 Sci. Forum 827, 174–179. https://doi.org/10.4028/www.scientific.net/MSF.827.174

364 28. Sosiati, H., Muhaimin, M., Purwanto, Wijayanti, D.A., Triyana, K., 2014. Nanocrystalline
365 Cellulose Studied with a Conventional SEM. 2014 Int. Conf. Physics, ICP 2014 12–15.
366 https://doi.org/10.2991/icp-14.2014.3

367 29. USDA, 2021. World agricultural production. Ekon. APK.

30. Zhang, Q., Lu, Z., Su, C., Feng, Z., Wang, H., Yu, J., Su, W., 2021. High yielding, one-step mechano-enzymatic hydrolysis of cellulose to cellulose nanocrystals without bulk solvent. Bioresour. Technol. 331, 125015. https://doi.org/10.1016/j.biortech.2021.125015

372

373 **Figure captions**

374 **Figure 1.** XRD spectra of (a) untreated and (b) delignified freeze dried cellulosic materials.

375 **Figure 2.** FTIR spectra of untreated (black), delignified freeze dried (blue) and after hydroly-
376 sis (red) (a) corn cob and (b) sawdust, (c) FTIR spectra of solid formed by freeze dried sam-
377 ples of the supernatant after: 24 h (black), 72 h (blue), 168 h (red) and 336 h (pink) of corn
378 cob's hydrolysis.

379 **Figure 3.** Porosimetry analysis of delignified cellulosic materials during their hydrolysis with
380 cellulase. (a) BET surface area (m^2/g), (b) Pore volume (BJH) (cm^3/g), (c) Pore size (BET)
381 (nm), (d) % pore volume between 2-70 nm of delignified freeze dried cellulosic materials dur-
382 ing their hydrolysis with cellulase enzymes.

383 **Figure 4.** (a) TEM image of hydrolyzed corn cob (solid part) after 24 h of hydrolysis, (b)
384 TEM image of solid formed by freeze-dried samples from supernatant after 72 h of corncob's
385 hydrolysis.

386 **Figure 5.** Process flow sheet with mass (kg) and energy (kg of steam) balance for CHNTs
387 production. 1. Delignification tank (100 m^3); 2. Enzyme production bioreactor (10 m^3); 3.
388 Sterile filter (150 m^3/min); 4. Air pump (150 m^3/min); 5. CHNTs production bioreactor (100
389 m^3/min); 6. Pump (4 m^3/h); 7. Centrifugal separator (20 m^3/h); 8. Tank for CHNTs solution
390 (100 m^3); 9. Condenser (3.3 m^3/h); 10. Freeze dryer – water removal (6000 kg/d); 11. Boiler
391 (2500 kg oil/day); 12. Pump (20 m^3/h); 13. Vacuum pump 5Hp

392

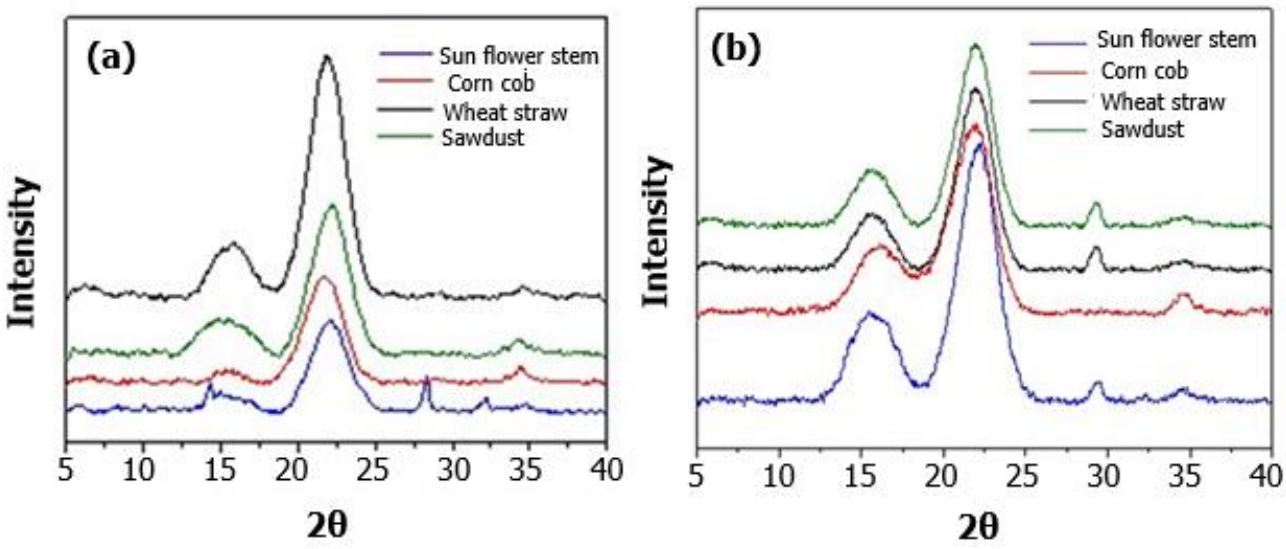

393
394 **Figure 1.**

395
396

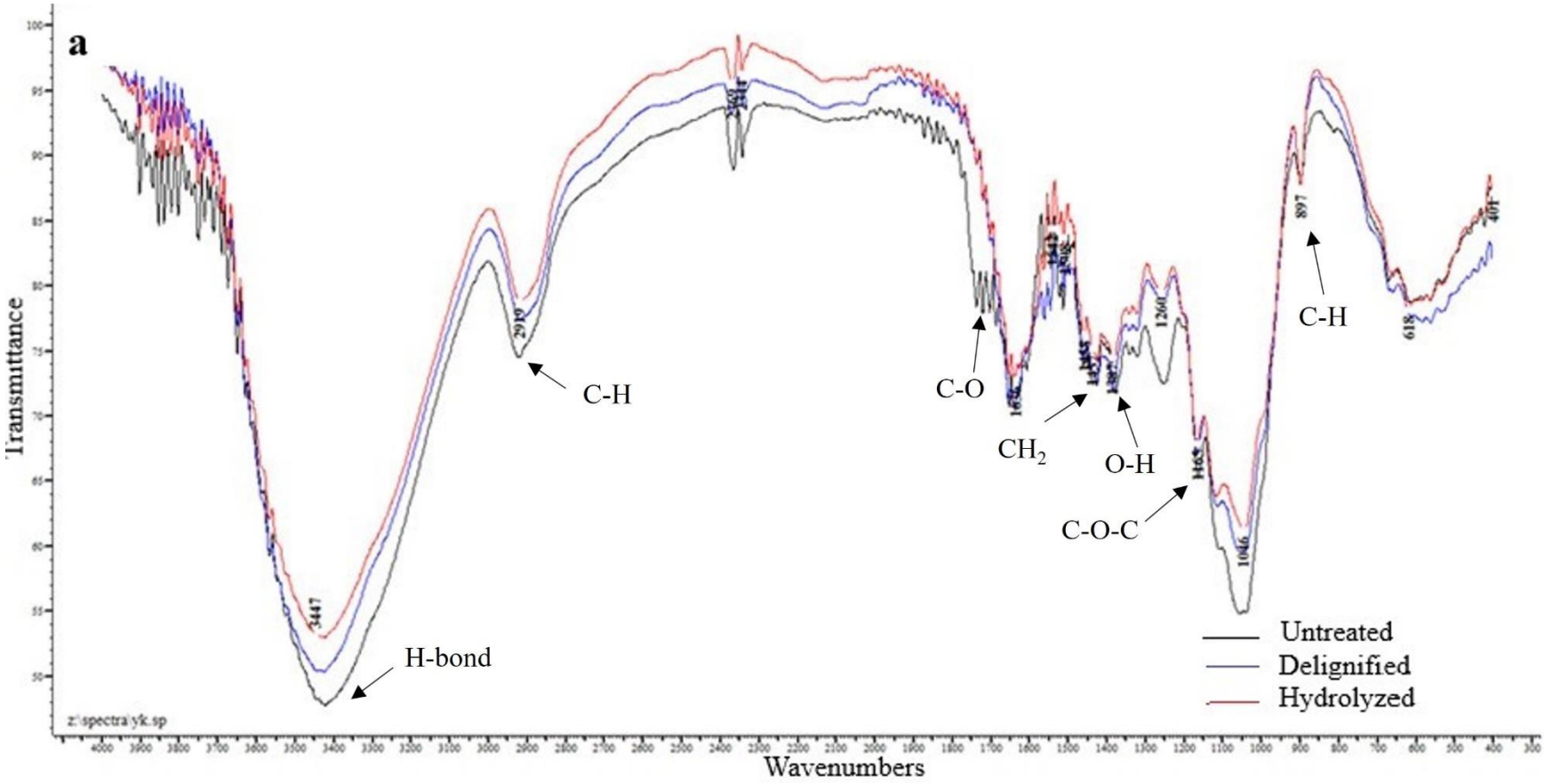
a
Transmittance
Wavenumbers
C-H
H-bond
C-O
CH2
O-H
C-O-C
C-H
Untreated
Delignified
Hydrolyzed

Figure 2a.

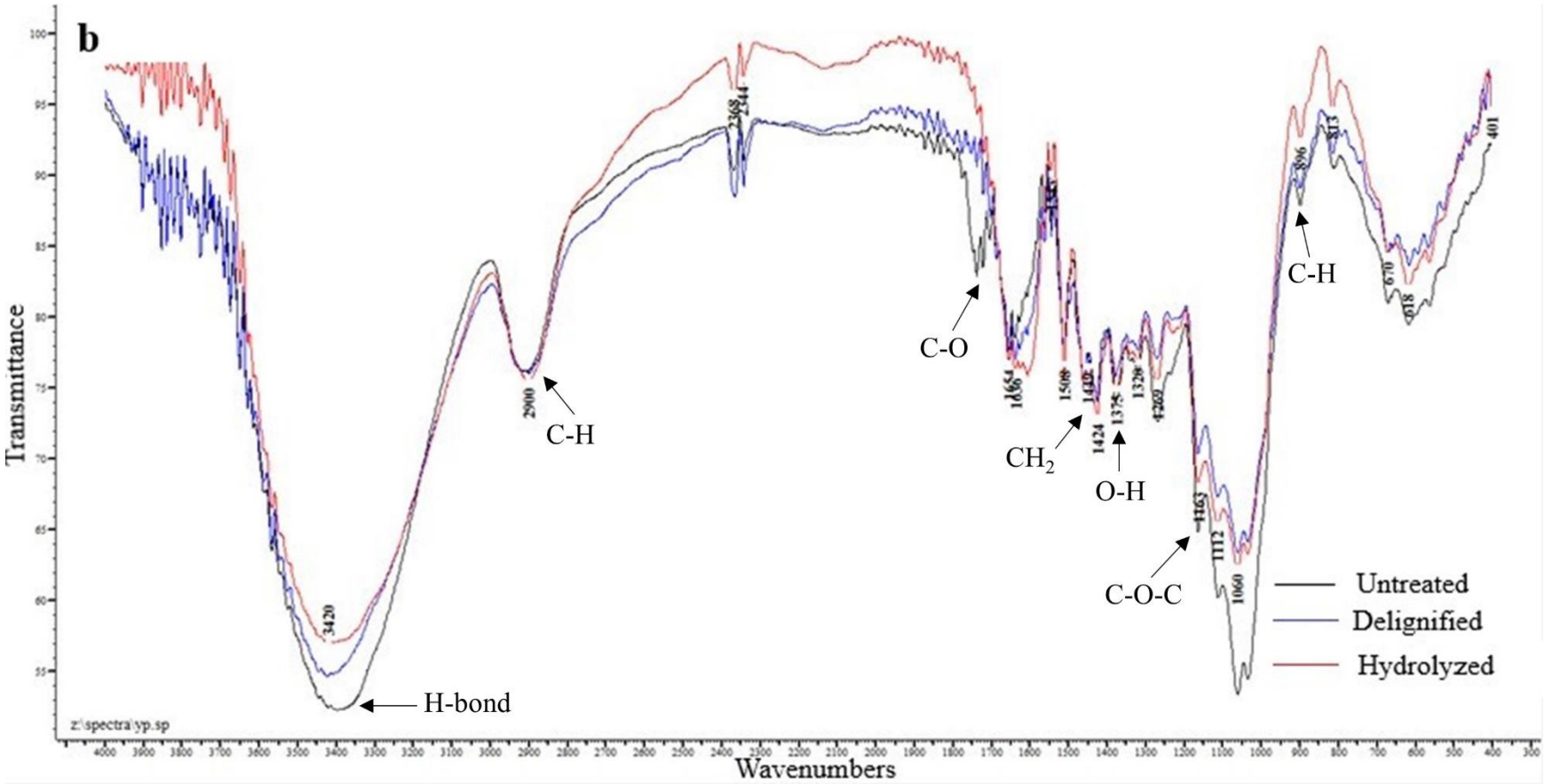
b
Transmittance
Wavenumbers
H-bond
C-H
C-O
CH2
O-H
C-O-C
C-H
Untreated
Delignified
Hydrolyzed
z:\spectra\yp.sp

Figure 2b.

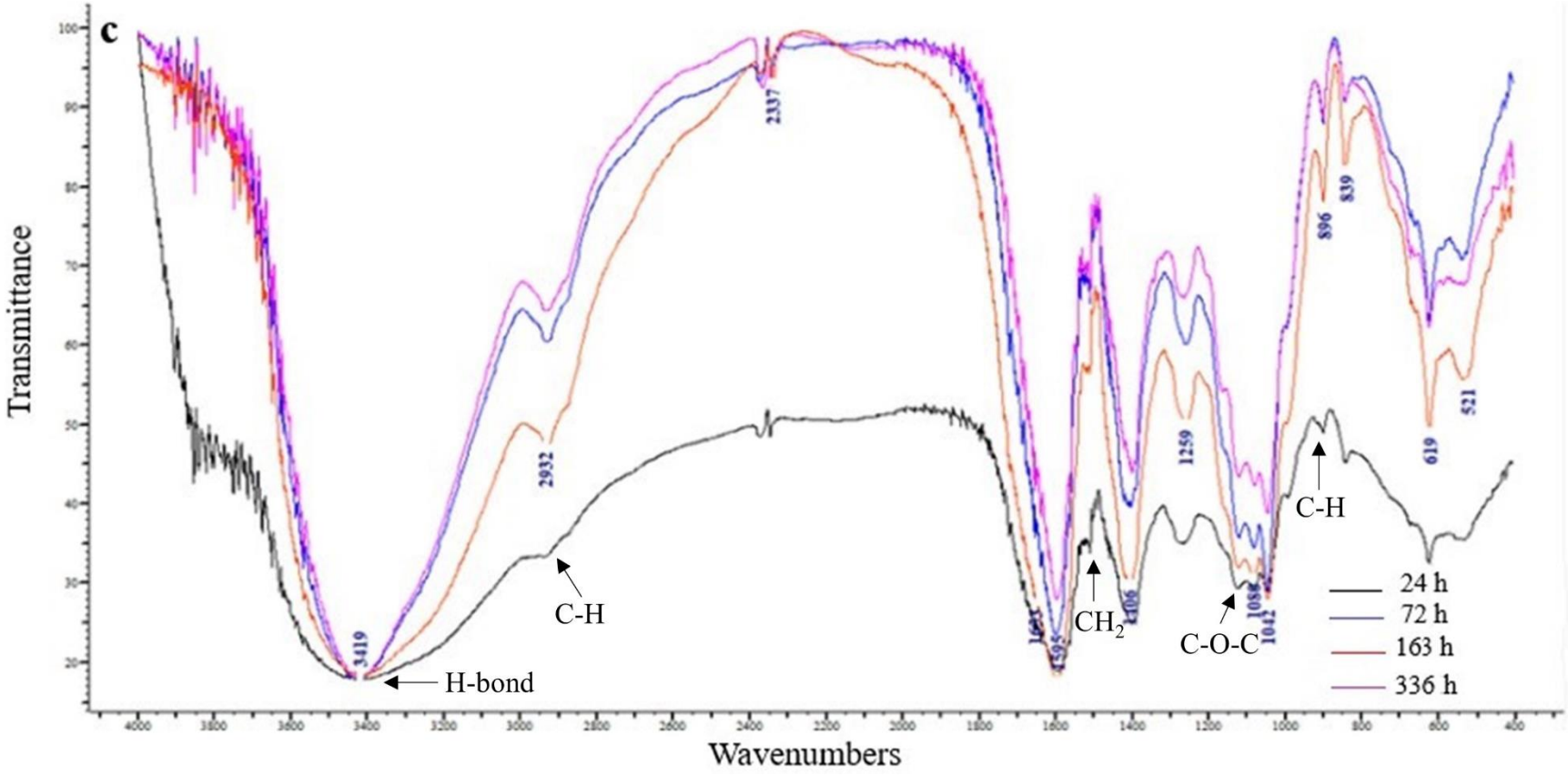
c
Transmittance
Wavenumbers
3419
2932
2337
1595
1259
1088
1042
896
839
619
521
H-bond
C-H
CH2
C-O-C
C-H
24 h
72 h
163 h
336 h

Figure 2c.

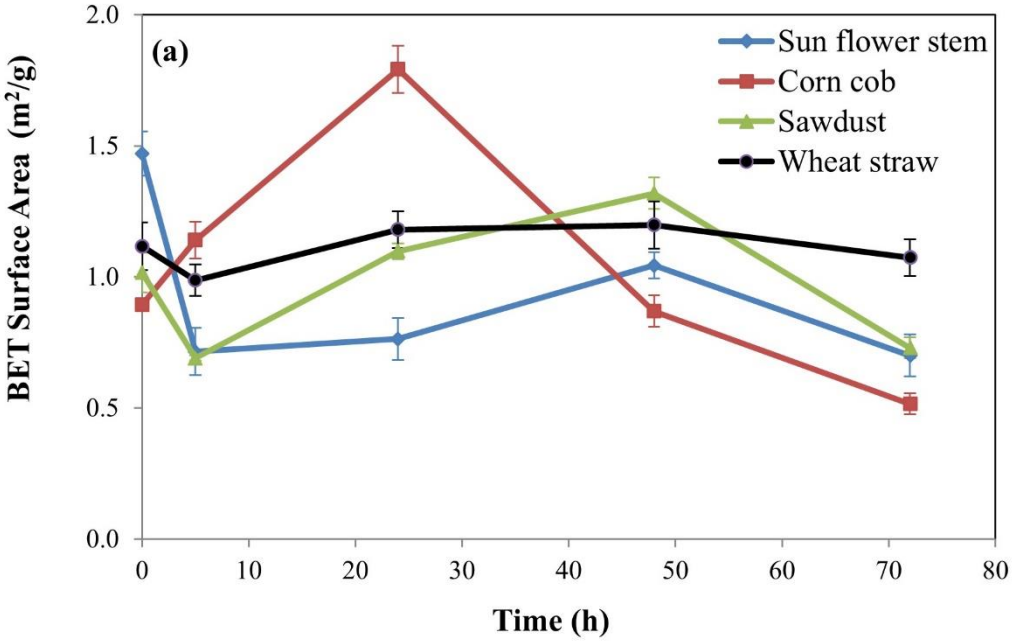
(a)
BET Surface Area (m²/g)
Time (h)
Sun flower stem
Corn cob
Sawdust
Wheat straw
2.0
1.5
1.0
0.5
0.0
0
10
20
30
40
50
60
70
80

Figure 3a.

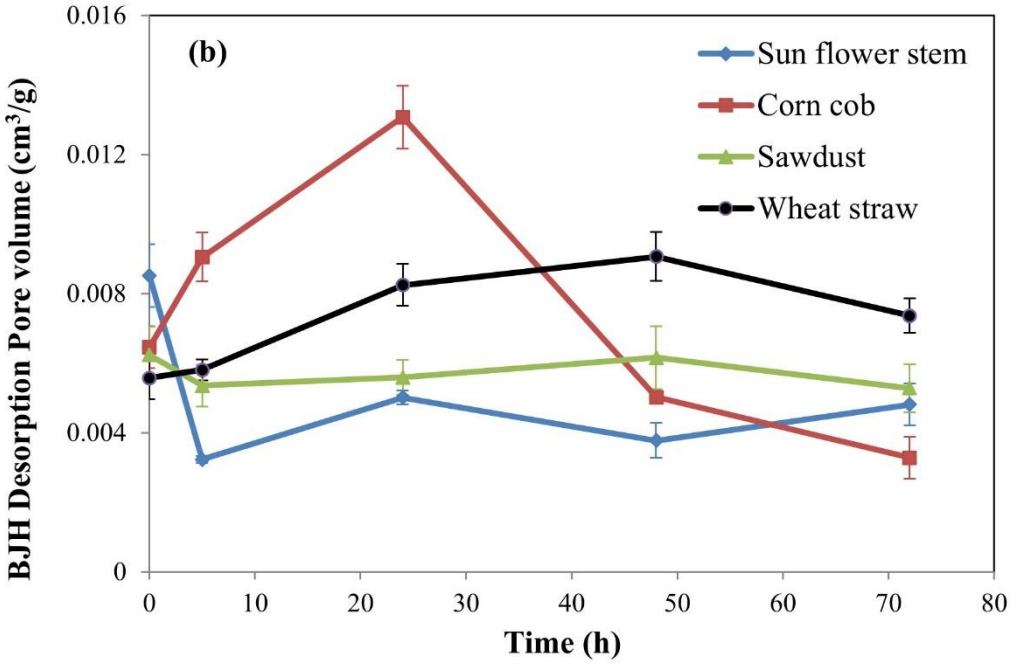
(b)
Sun flower stem
Corn cob
Sawdust
Wheat straw
BJH Desorption Pore volume (cm3/g)
0.016
0.012
0.008
0.004
0
0
10
20
30
40
50
60
70
80
Time (h)

Figure 3b.

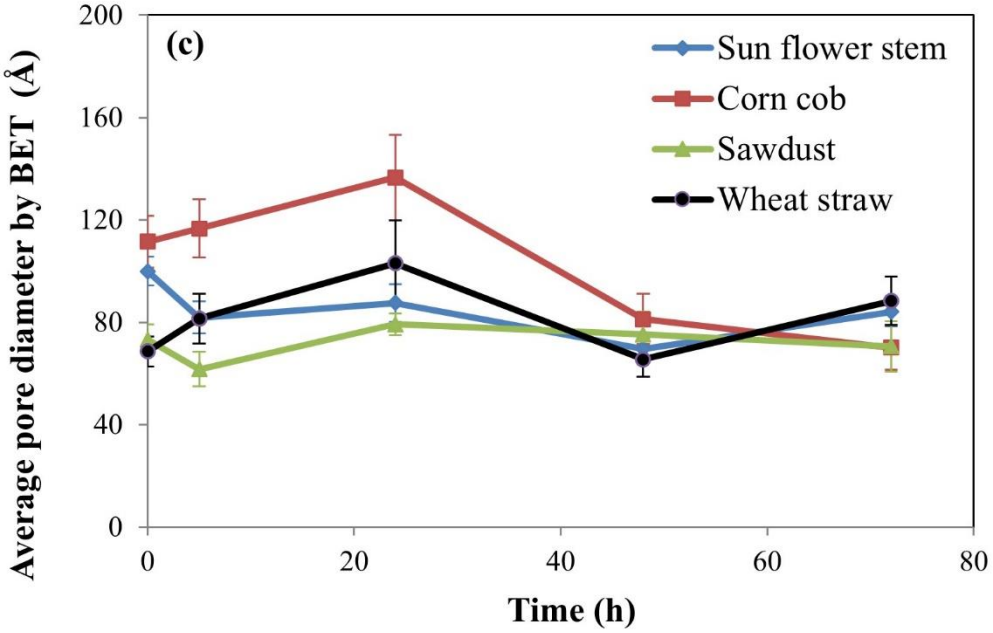
(c)
Sun flower stem
Corn cob
Sawdust
Wheat straw
Average pore diameter by BET (Å)
Time (h)
200
160
120
80
40
0
0
20
40
60
80

Figure 3c.

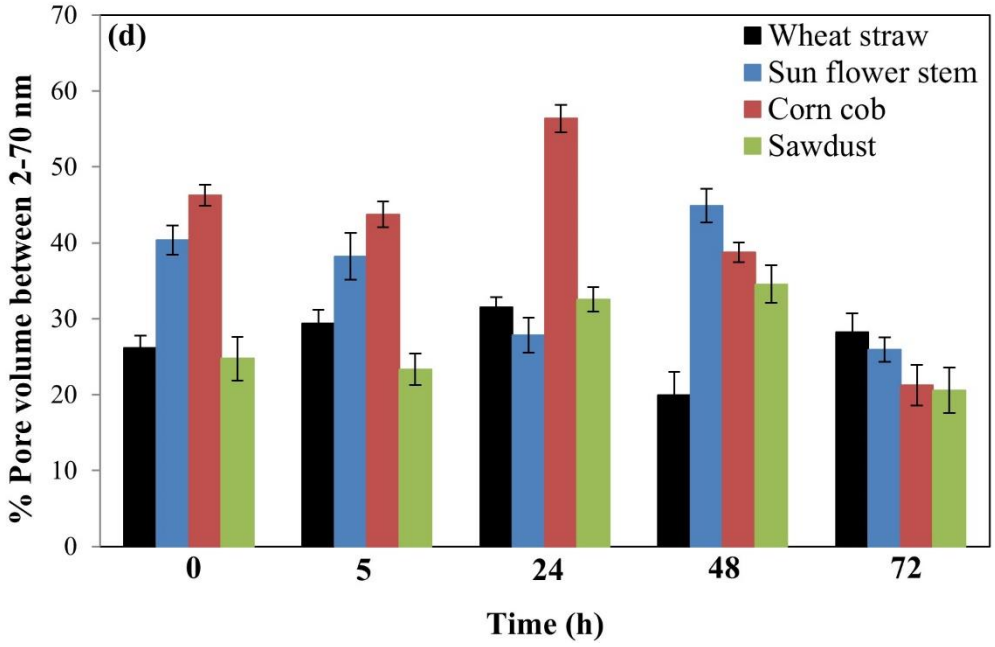
(d)
Wheat straw
Sun flower stem
Corn cob
Sawdust
% Pore volume between 2-70 nm
70
60
50
40
30
20
10
0
0
5
24
48
72
Time (h)

Figure 3d.

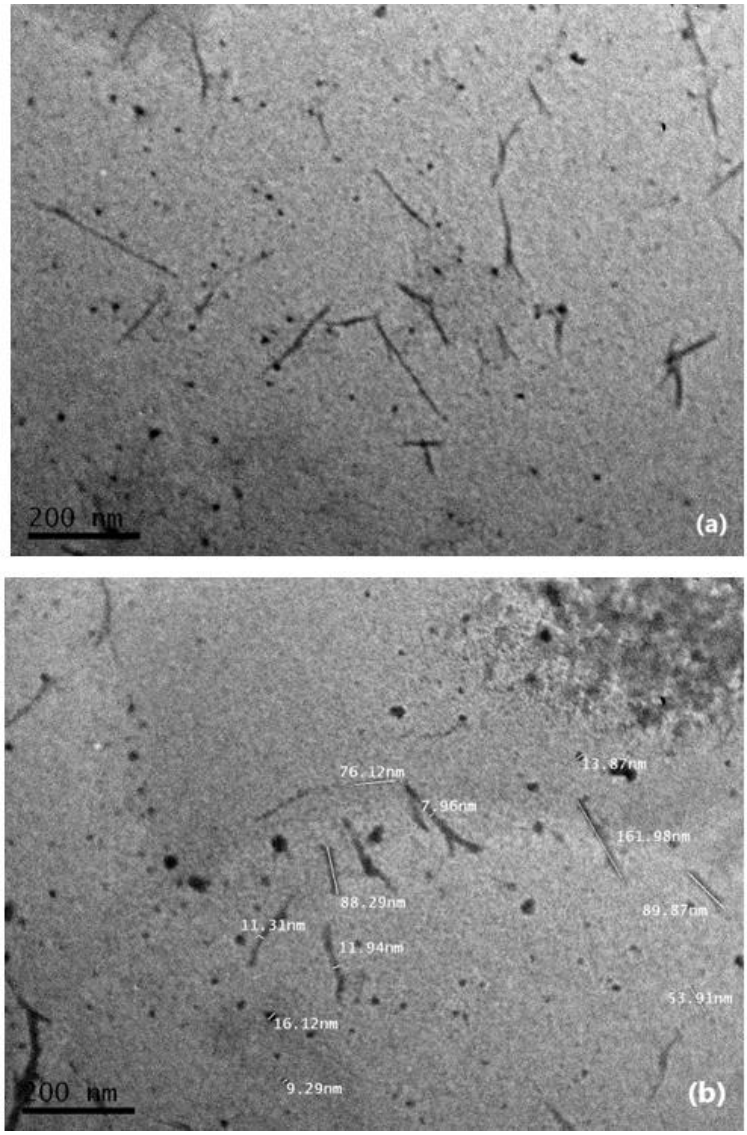
200 nm
(a)
76.12nm
13.87nm
7.96nm
161.98nm
88.29nm
89.87nm
11.31nm
11.94nm
53.91nm
16.12nm
9.29nm
200 nm
(b)

Figure 4.

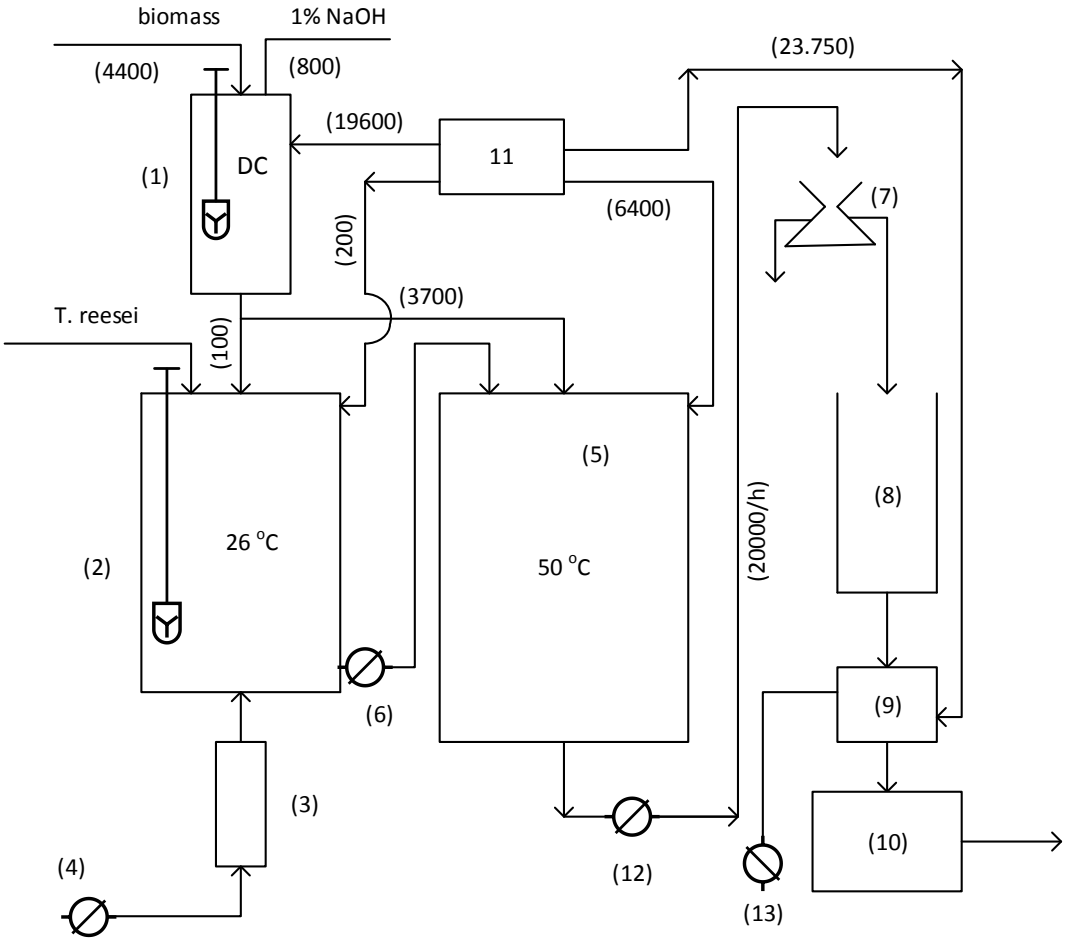

485 **Figure 5.**

486

487 **Table 1.** Porosimetry analysis of untreated and delignified freeze dried (TC) cellulosic materi-
488 als.
489

	BET Surface area (m^2/g)		**Pore volume$_{(BJH)}$ (cm^3/g)**		**Pore size$_{(BET)}$ (nm)**	
Cellulosics	Untreated	TC	Untreated	TC	Untreated	TC
Wheat straw	0.48 ± 0.01	1.12 ± 0.09	0.0034 ± 0.0006	0.0056 ± 0.0006	8.23 ±0. 95	6.85± 0.8
Sun flower stem	1.70 ± 0.08	1.47 ± 0.09	0.0060 ± 0.0008	0.0085 ± 0.0009	6.41 ± 0.97	9.99 ± 1.00
Corn cob	0.34 ± 0.02	0.89 ± 0.01	0.0026 ± 0.0004	0.0065 ± 0.0006	8.78 ± 0.82	11.14 ± 1.32
Sawdust	0.60 ± 0.02	1.02 ± 0.08	0.0033 ± 0.0007	0.0062 ± 0.0008	4.48 ± 0.64	7.33 ± 0.89

490 **Table 2.** Crystallinity degree and crystallite size of untreated, delignified (TC) and hydro-
491 lyzed freeze dried cellulosic materials.

Cellulosics	**Percentage of crystallinity (%)**			**Crystal size (nm)**		
	Untreated	TC	Hydrolyzed	Untreated	TC	Hydrolyzed
Wheat straw	53.0	61.6	66.5	31.7	3.3	3.9
Sunflower stem	66.2	57.7	61.9	31.2	3.0	3.8
Corn cob	45.3	58.0	61.6	30.7	3.1	3.6
Sawdust	56.6	60.8	59.5	30.4	3.3	3.5

492

493 **Table 3.** Porosimetry analysis of freeze dried samples from supernatant during corn cob's hy-
494 drolysis with cellulase.

495

	BET Surface area (m^2/g)	**Pore volume$_{(BJH)}$ (cm^3/g)**	**Pore size$_{(BET)}$ (nm)**
24 h	0.79±0.03	0.0040±0.0001	3.60 ± 0.2
72 h	1.35±0.1	0.0069±0.0005	4.60 ± 0.6
168 h	0.20±0.009	0.0011±0.0003	1.65 ± 0.3
336 h	0.35±0.04	0.0025±0.0002	1.60 ± 0.3

496

497 **Table 4.** Investment cost. Equipment cost for plant installation.

Machinery	**Capacity**	**Price (€)**
Delignification tank	100,000 L	30,000
Enzyme production bioreactor	10,000 L	20,000
Sterile filter	150 m^3/min	9,000
Air pump	150 m^3/min	20,000
CHNTs production bioreactor	100,000 L	30,000
Pump	4 m^3/h	2,000
Centrifugal separator	20 m^3/h	150,000
Tank for CHNTs solution	100,000 L	30,000
Condenser	3.3 m^3/h	300,000
Freeze dryer	6000 Kg water/day	500,000
Boiler	2500 Kg oil/day	600,000
Pump	20 m^3/h	2,000
Vacuum pump	5 HP	20,000
Pipe lines		30,000
Total		1,743,000

498 **Table 5.** Daily Production Cost. Parameters affecting the production cost.

499

Parameter	Cost (€/day)
Raw material	400
Labor cost	1,070
Thermal energy	830
Electricity	35
Water requirement	40
Consumables	205
Investment payments	156
Total	2731

Carbohydrate Nano-tubes Production and its Techno-economic Validation

Athanasia Panitsa[a], Theano Petsi[a], Eleana Kordouli[a], Poonam Singh Nigam[b], Maria Kanellaki[a], Athanasios A. Koutinas[a*]

[a] Food Biotechnology Group, Department of Chemistry, University of Patras, Patras, Greece.

[b] Biomedical Sciences Research institute, Ulster University, Coleraine, N. Ireland, UK.

sissy_panitsa@hotmail.com, thpetsi@upatras.gr, ekordouli@upatras.gr, p.singh@ulster.ac.uk, M.Kanellaki@upatras.gr, A.A.Koutinas@upatras.gr

**Corresponding author*

Tel:0030.2610.997104 e-mail:A.A.Koutinas@upatras.gr

Style Definition: TA_Main_Text

ABSTRACT

The p~~P~~roduction of carbohydrate~~-~~nano~~-~~tubes (CHNTs) using agricultural wastes is proposed in this investigation. The corncob was found to be the most productive for our purpose among the four lignocellulosic raw materials tested. CHNTs production was accomplished in two stages. Tubular ~~Cellulose~~ cellulose (TC) was prepared from raw substrates through a delignification process, and the prepared tubes of TC were cut~~-~~ ~~to~~into nano-size carbohydrate~~-~~tubes in a chemical-free process. To achieve this, cellulase was produced in our lab using agricultural residue, employing ~~a high cellulase producer~~ the non-pathogenic ~~fungi~~ fungus *Trichoderma reese~~i~~.* a high cellulase producer. Analysis of the produced CHNTs proved stability, nano~~-~~dimension lengths, and increased crystallinity. The technoeconomic feasibility report showed that the production of CHNTs is cost-effective. This was supported by a process flow sheet with mass and energy balances based on laboratory experimental results.

KEYWORDS: *corncob; cellulose; Trichoderma reesei; cellulase; hydrolysis; Carbohydrate nano~~-~~tubes.*

1. Introduction

Over the past few decades, nanotechnology, nano-synthetic materials, and their applications have gained attention. Carbon ~~Nano Tubes~~ nanotubes(CNTs) are among the most commonly used nano-materials. These CNTs are rolled graphene with sp^2 hybridization and can be divided into three categories, according to the number of tubes present in CNTs: single-walled CNTs, double-walled CNTs, and multi-walled CNTs (Eatemadi et al., 2014; Ibrahim, 2013). Information on CNTs was first published in 1991 (Lijima, 1991), and since then this nano-material has established rapidly growing applications in sensors, nano-medicine, environment, energy, and others (Ibrahim, 2013). However, their use in the biological and biomedical sectors ~~for~~ of the human system is restricted due to their increased toxicity to the human body. The size of nanotubes can affect the toxicity of CNTs, particularly those with a size under 100 nm. They can affect the lungs and whole respiratory system by activating immunological responses~~,~~ modifying protein structure, and these re-disperse from their site of deposition in the human system (Eatemadi et al., 2014; Satishkumar et al., 2000). ~~The p~~Prolonged and excessive exposure to CNTs can cause inflammation and oxidative stress (Nemmar et al., 2001).

In order to avoid the side effects ~~–~~of CNT use, we anticipated that alternative agricultural materials~~,~~ could be used for nanotubes production. Inexpensive and renewable natural resources were explored for the production of carbohydrate nano-tubes (CHNTs). Such materials can be made from residual plant~~s~~ stalks, which are generated as by-products of each crop. Globally, enormous amounts of agricultural waste, such as wheat straw, sunflower stems, and corncobs, are produced each year following the harvesting of wheat grains, corn, and sunflower seeds. (Barouni et al., 2015; Bian et al., 2018; Cavali et al., 2020; Chen et al., 2021; FAO, 2019; Koutinas et al., 2016a; USDA, 2021). Nanofibers produced from natural cellulosic waste materials and their application in nanocomposite materials ~~is a topic of~~are topics in Green-Advance. The advantages of cellulose nanofibers include their biodegradability, biocompatibility, renewable nature, high strength and stiffness, and low weight. (Kumar et al., 2020; Reddy and Rhim, 2014; Sosiati et al., 2014). Furthermore, nanocellulose's structure can be modified to meet the needs of particular applications by not only using a particular agricultural product as the ma-

terial's initial carbon source but also by improving or changing the method of production. Nanocelluloses have ~~proved~~ proven to be possible fillers for the improvement of the mechanical properties of biopolymer films, such as starch, alginate, and chitosan films (Barouni et al., 2015; Koutinas et al., 2016a; Kumar et al., 2020; Reddy and Rhim, 2014; Shankar and Rhim, 2016). Our previous studies have shown that lignocellulosic material after delignification~~,~~ can be used for the formation of tubular cellulose~~,~~ with micro and nano dimensions (Koutinas et al., 2016b). The aim of this work was the production of carbohydrate~~-~~nanotubes (CHNTs), a new generation of nano~~-~~tubes, from the carbon content of agricultural residues via the preparation of tubular~~-~~cellulose (TC) in an enzymatic process.

2. Experimental

2.1 Agricultural residual materials

In our experiments, we used free or low-cost materials such as corncob and sunflower stems from local farms, wheat straw from a local cattle feed market, and sawdust from a local timber mill.

2.2 Cellulase preparation

For a g~~G~~reen, economical technology, we used cellulolytic enzymes prepared in our lab from carbon sources of agricultural origin. A high cellulase-producer, *Trichoderma reesei* (ATCC 26921), was grown on Potato Dextrose Agar (PDA) medium at 30 °C for 5-7 days. Fungal spores were aseptically collected from the surface of PDA plates~~,~~ by gently scraping with sterilized water and were counted on a hemocytometer (Neubauer Improved, HBG, Germany). The production of cellulase was carried out using a modified method ~~of~~ by Li et al. (2013). Two mL of spore suspension containing 10^6-10^7 spores mL^{-1} was precultured in 60 mL of sterilized medium consisting of 2%~~,~~ w/v delignified sawdust, 1% soy peptone, and 1% glucose. The pH of the medium was adjusted ~~at~~ to 4.5 with a 2M NaOH solution and incubated in a VELP Scientifica FOC incubator at 30 °C and 180 rpm for 24 h. Forty mL of freshly grown preculture was aseptically added into a 2 L bioreactor (Electrolab), containing 1 L of sterilized medium made of 25 g delignified sawdust, 1.7% soy peptone, 0.5% $(NH_4)_2SO_4$, 0.6% KH_2PO_4, 0.2% $MgSO_4 \cdot 7H_2O$, 0.25% glycerol, and 2 mL Tween 20. The bioreactor equipped with the control devices Fermac 231/260 was operated at 26 °C, 300 rpm, ~~ventilation~~ 1.5 L/min ventilation and

pH 4.5—5.0. After 150 h of fungal growth, the content was aseptically centrifuged to obtain a clear supernatant for use as a crude preparation of cellulolytic enzyme.

2.3 Assay of cellulase activity

One mL of crude enzyme (prepared as above) was mixed with 100 mL of sodium citrate buffer (pH 5.0). From this, 5 mL was placed in a 50 mL conical flask with 10 mL of buffer and 0.5 g of finely stripped Whatman filter paper. The reaction- mixture was incubated at 50 °C for 60 min, and the released glucose due to enzyme activity was measured by High Performance Liquid Chromatography (HPLC) on a Shimadzu LC-9A. Enzyme units were calculated against a standard curve plotted for glucose released in a similar reaction conducted with a commercial cellulase with known units (Chu et al., 2012).

2.4 Stage-1 Preparation of tubular cellulose (TC)

Lignocellulosic materials, including corncob, sunflower stem, wheat straw, and sawdust, were subjected to a very mild (1%, w/v) NaOH solution treatment for three hours at 70 °C. Materials were filtered out and washed with hot (90 □ -95 □) deionized water for complete removal of NaOH and released lignin. The delignified material produced in this procedure was employed as TC in a later stage; therefore, it was freeze-dried at 15×10^{-3} mbar and -45 °C using a Labtech Daihan Freeze Dry System.

2.5 Stage-2 Enzymatic treatment of TC to develop CHNTs

In separate flasks containing 200 mL of buffer pH 5.0 and 10 mL of crude enzyme, 15 g of TC prepared from four agricultural residues were incubated at 50 °C for 72 hours without stirring or mixing. ~~Fifteen g each of TC prepared from four agricultural residues material were placed in separate flasks, with 200 mL of buffer pH 5.0 and 10 mL of crude enzyme and incubated at 50 °C for 72 h, without any stirring or mixing.~~ To examine the formation of CHNTs samples from the flasks of each substrate were taken at 5, 24, 48, and 72 h intervals.

2.6 Stage-3 Isolation of CHNTs

After hydrolysis of TC ~~an amount~~ a quantity of clear supernatant liquid ~~and~~ without dispersed solids was taken ~~,~~ in order to isolate ~~the CHNTs soluble in~~ the water-soluble CHNTs. The liquid was freeze-dried, and porosimetry and TEM analysis were performed in the ~~received~~ powder received.

2.7 Examination of CHNTs

Following all Standard Operating Procedures (SOPs) for each equipment used, examination of CHNTs ~~were~~ was conducted as below: ~~specific~~ Specific surface area, pore size distribution, and pore volume of all types of materials (original raw material, TC, and CHNT) was carried out by N_2 adsorption-desorption process at -196.15 °C on a Tristar 3000 porosimeter (Micromeritics); Jeol Model JSM-5600LV scanning electron microscope was used operating at an accelerating voltage of 20 kV; X-ray powder diffractometry (XRD) was used to test the crystallinity of materials on a Bruker AXS D8 ADVANCE at 40 kV and 20 mA. Segal's equation based on the diffraction pattern intensity was used for the calculation of the crystallinity index (CI). Transmission Electron Microscopy (TEM) images were taken with the help of a Gatan~~,~~ model 782 Erlangshen E5500W camera. FTIR spectra of samples were obtained using a FTIR Perkin-Elmer spectrophotometer, 16 PC model, in the range of 4000–400 cm^{-1}.

2.8 Technoeconomic validation and Process Flow Sheet for industrial application

Details of the process flow sheet design ~~is~~ are presented in Figure 5, and the investment and daily production costs are presented in Tables 4 and 5, respectively. The delignification of biomass takes place in~~to~~ tank 1, by supplying steam ~~by~~ through a boiler (11) and the delignified cellulosic material is transferred to enzyme production bioreactor (2) and CHNT~~s~~ production bioreactor (5). The enzyme production bioreactor (2) is supplied with air by an air pump (4) through a sterile filter (3). The temperature in bioreactors 2 and 5 is kept constant at 26 □ and 50 □ respectively, by supplying steam from the boiler (11). The hydrolysate from the bioreactor 5 containing CHNTs is pumped to the centrifugal separator (7) to separate suspended solids from the solution of CHNTs. A clear CHNTs solution is collected in tank 8, then concentrated in a condenser (9), and subsequently ~~is~~ freeze-dried in a freeze-dryer system (10).

Formatted: Font: Not Bold

3. Results and Discussion

3.1 Structure of TC

From the SEM images (Fig. S1) of wheat straw, sunflower stem, corncob, and sawdust (original and delignified), it can be observed that the morphology of the materials ~~was~~ changed after delignification, pores were created on the surface of the materials, and the fibers arranged in TC could be seen (Fig. S1~~ref supplementary materials~~). These changes are attributed to the removal of amorphous areas, which was earlier occupied by lignin and hemicellulose contents in raw substrates (Cavali et al., 2020). The two naturally occurring forms of cellulose are Iα and Iβ. In this analysis, only Iβ was visible, as it is part of higher plants, in contrast to the form Iα only found in bacterial and algae celluloses (Poletto et al., 2014). Studies of atomic resolution synchrotron and neutron diffraction data, have shown that cellulose Iα has a triclinic unit cell P1 ($a = 6.717$ Å, $b = 5.9962$ Å, $c = 10.400$ Å, $\alpha = 118.08°$, $\beta = 114.80°$, and $\gamma = 80.37°$) containing a single cellulose chain, while ~~that~~ cellulose Iβ has a monoclinic unit cell P21 ($a = 7.784$ Å, $b = 8.201$ Å, $c = 10.380$ Å, $\alpha = \beta = 90°$, $\gamma = 96.5°$) containing two conformationally distinct cellulose chains, called original chains and central chain (Krichen et al., 2022). The structure of cellulose Iβ is mainly in the form of parallel chains linked by H-bonds stacked with an alternating shear parallel to the chain axis stabilized by Van der Waals interactions (Poletto et al., 2014). After delignification of materials, the specific surface area of TC (Table 1) was about 2-fold higher due to the formation of cellulose tubes in the space created by the removal of lignin fraction. The pore volume and pore size were also increased, except for TC prepared from sunflower stem, which had a lower specific surface area (Table 1).

3.2 Crystallinity analysis

The degree of cellulose crystallinity plays an important role in cellulose structure parameters. Since the crystal structure of cellulose affects the enzymatic ~~-~~hydrolysis (Park et al., 2010), the crystallinity was examined in XRD analysis (Fig. 1 and Table 2). The characteristic peaks of Iβ cellulose were observed at 2θ (theta) of about 16º, and 22.64º (Banvillet et al., 2021; Bian et al., 2018; Ling et al., 2021;

Zhang et al., 2021). The sharper peaks in the XRD profile of TC materials indicate that ~~its~~ their degree of crystallinity was higher compared to that of the raw materials. For delignified sawdust, sunflower stem, and wheat -straw, a peak located at 2θ of about 30.0° was also identified. This can be an indication of amorphous areas after delignification (Sosiati et al., 2015; Sosiati and Harsojo, 2014). Another characteristic peak of cellulose Iβ at 2θ of about 35.0° appeared for all materials (Banvillet et al., 2021; Ling et al., 2021; Zhang et al., 2021). An increase in the rigidity of cellulose tubes (fibers) and a decrease in their flexibility occur~~s~~ when there is an increase in the ratio of crystalline to ~~/~~amorphous regions. Sunflower stem and corn cob had the lowest crystallinity indices (CI) (Table 2). CI increases as the surface area of the crystallites corresponds to decrease in amorphous cellulose, due to the void spaces available after lignin removal (Cavali et al., 2020; Poletto et al., 2014).

3.3 FT-IR spectra

The spectra for corncob and wheat-straw are presented in Figs. 2a and 2b, for the other two materials, spectra were similar (hence not presented here). At around 3440-3420 cm^{-1} an intramolecular H-bond vibration appeared, which indicates cellulose (Poletto et al., 2014). The FTIR absorption peaks at ~2900 cm^{-1} are characteristic of the stretching vibration of C-H groups of cellulose (Reddy and Rhim, 2014). The absorption peaks at 1440-1430 cm^{-1} are due to CH_2 bending vibration and indicate~~s~~ the "crystallinity band" in the cellulose. A reduction or/ expansion in the intensity of this crystallinity band among the untreated, delignified freeze dried, and after enzymatic hydrolysis samples indicates that the level of crystallinity of cellulose crystals decreased/increased during treatment -processes (Shankar and Rhim, 2016). The peaks appeared at 1375 cm^{-1} are typical of the O-H bending vibration of cellulose. The peaks at 1163-1165 cm^{-1} are attributed to the C-O-C pyranose ring stretching vibration and the peaks at 896-898 cm^{-1} indicate the C-H rocking vibration of cellulose present in the microfibers and nanofibers (Reddy and Rhim, 2014). No considerable changes in the absorption peak~~s~~ positions of untreated and delignified freeze--dried samples (TC), were observed (Figs. 2a and 2b), which indicated that these processes did not alter the chemical structure of the cellulosic materials. However, the spectra bands present at around 1730 cm^{-1} in raw lignocellulosic (due to C-O stretching vibration for the acetyl and ester linkages in lignin/hemicellulose) were absent in the spectra of TC. That confirmed the

absence of lignin and hemicellulose in TC, which were removed in stage -1 of alkali treatment (Gabriel et al., 2020; Kargarzadeh et al., 2012; Kumar et al., 2020).

3.4 Enzyme- treatment of TC for development of CHNTs

TC materials were treated with our lab-prepared crude cellulase (70 FPU/g) to develop CHNTs. N_2 adsortion-desorption porosimetry analysis (Figs. 3a, b, c) show the kinetics: BET surface area (m^2/g) and pore volume are given by BJH equation, and the pore size by BET (nm). CHNTs were produced after 24 h enzyme treatment of TC obtained from four agricultural- substrates. CHNTs from corn cob presented the highest value of surface area (1.8 m^2/g), which is a desired parameter for the entrapment of pharmaceutical substances, food preservatives, and other entities in CHNTs (Panitsa et al., 2021). Based on the number of tubes with pore widths between 2-70 nm (Fig. 3d) in combination with pore-volume (0.013 cm^3/g) and the average pore diameter (13.5 nm), corncob-TC proved to be the most productive material among the TC of other substrates, for the development of CHNTs.

3.5 Physicochemical properties of the isolated CHNTs product

CHNTs retain some important properties of cellulose, such as biodegradability and non-toxicity. CHNTs are oligomers ~~having~~ with glucose as their structural unit~~,~~ and can form hydrogen bonds with OH groups containing enzymes and drugs. The characterization of the isolated product of CHNTs was carried out by TEM to prove the nano-dimensions of the length of tubes. Porosimetry analysis confirmed the pore size (Table 3) and pore distribution (Fig. S3), classifying the material ~~in~~ a nanomaterial~~s~~.

3.5.1 Transmission Electron Microscopy of the isolated CHNTs product

TEM images of CHNTs developed from corncob showed needle-like cellulosic nanotubes (Fig. 4 a,b) with an internal diameter 6-16 nm and a length of tubes in the range of 80-160

nm. These data proved that the cellulosic tubes in TC after ~~the~~ treatment with cellulolytic enzymes produced carbohydrate nanotubes ~~CarboHydrate Nano Tubes~~ (CHNTs).

3.5.2 Porosimetry analysis of the isolated CHNTs product

The BET surface area was 1.35 m^2/g and the pore width was 4.6 nm after 72 hours of hydrolysis, as shown in Table 3 (~~supplementary materials~~). Porosimetry measurement revealed an average pore diameter (tube diameter) of around 4-5 nm (Fig. 4b), which is consistent with the size of the tubes depicted in the TEM image. ~~Table 3 shows that after 72 h of hydrolysis, the pore width was 4.6 nm with a volume of 0.0069 cm^3/g and a BET surface area of 1.35 m^2/g (ref supplementary materials). The average pore diameter (tube diameter) of about 4-5 nm measured with porosimetry analysis is comparable with the size of tubes shown in the TEM image (Fig. 4b).~~

3.6 Design and operation of the bioreactor and economic validation of technology

The bioreactor system presented in Figure 5 contains ~~the~~ bioreactor 2 of 10,000 L for enzyme production and ~~the~~ bioreactor 5 of 100,000 L for tubular cellulose (TC) hydrolysis to nano-tubes. Machineries of high cost are the condenser (9), freeze dryer (10) and centrifugal separator (7). The boiler (11) of 850 ~~litres~~ liters of oil per ~~/~~day and the delignification tank (1) are also of importance. Delignification tanks (1) and condensers (9) need about 87% of steam consumption. Centrifugal separators (7) and freeze dryers (10) need more ~~of~~ than 90% electricity consumption. The total investment cost has been calculated ~~to~~ at ~~€1,743,000 with~~1,743,000 with the bigger cost to be that of condenser (€300,000), freeze dryer (€500,000) and boiler ~~of~~ (€600,000). The parameters considered for the calculation of the daily production cost were raw material cost, labor, thermal energy, electricity, water requirement, consumables, and investment payment costs. The biggest costs are the labor cost and that of thermal energy, which are about 70% of the €2,731 ~~-~~daily cost. ~~-~~On the other hand, the annual turnover is equal

Formatted: Font: (Default) Times New Roman, 12 pt, Kern at 10.5 pt

Formatted: Superscript

Formatted: Highlight

to about €1,500,000, which could give a profit of €300,000 annually. So, it is estimated that the payment of investment costs will be achieved in about 6 years. This short period of investment repayment shows that the technology has a large margin of profit to convince the investors to proceed.

3.7. Technological and scientific implications

The aforementioned presentation of results and discussion have demonstrated the production of CHNTs. Specifically, the XRD and FTIR analysis proved that the tubes consist of cellulose, while lignin and hemicelluloses have been removed. They also proved the increment of crystallinity indices, which is related ~~with~~ to the rigidity of tubes. The formation of a new generation of tubes~~,~~ could lead to the preparation of a carrier material potentially usable as a drug delivery system. The metabolism and safety of CHNTs in the human body should be examined. Immobilization of cellulase in CHNT tubes with pharmaceutical substances could be considered ~~as~~ a possible method for removing the carrier material~~,~~ from the body, after its action. Cellulase, has the ability to hydrolyze cellulose into glucose, a nutrient for humans. Finally, the method of producing CHNTs is feasible, and the raw material is sustainable. The technoeconomic validation based on laboratory results showed that the process is cost–effective. This is supported by laboratory results (~~ref see supplementary material~~Table S1).

4. Conclusions

The Technoeconomic feasibility report validated that CHNT~~s~~ production is cost-effective. A ~~Green~~ green technology ~~was used, using~~was applied for four agricultural- residual materials. Among them, corncob has proved the most productive. It is free ~~of cost~~, making our process economically viable. TC tubes from corncob were cut short with cellulase, a cheaper lab preparation from *Trichoderma reesei*, to carbohydrate tubes of nano-size. FTIR and XRD analysis revealed the stability of CHNT's chemical structure. CHNTs were isolated from the solution of ~~hydrolysed~~hydrolyzed cellulose after

Formatted: Font: Not Bold

Formatted: Highlight

Formatted: Highlight

freeze-drying. The nano-dimension tubes of the final product were confirmed by TEM and ~~with~~ porosimetry analysis. CHNTs-based ~~a~~ carrier materials could potentially be used as drug delivery systems. However, their metabolism in the human body should be studied for their safety.

E-supplementary data for this work can be found in e-version of this paper online

.

Acknowledgements

We acknowledge support of this work by the project "Research Infrastructure on Food Bioprocessing Development and Innovation Exploitation – Food Innovation RI" (MIS 5027222), which is implemented under the Action "Reinforcement of the Research and Innovation Infrastructure", funded by the Operational Programme "Competitiveness, Entrepreneurship and Innovation" (NSRF 2014–2020) and co-financed by Greece and the European Union (European Regional Development Fund).

Funding

This work was supported by the project "Research Infrastructure on Food Bioprocessing Development and Innovation Exploitation – Food Innovation RI" (MIS 5027222), which is implemented under the Action "Reinforcement of the Research and Innovation Infrastructure", funded by the Operational Programme "Competitiveness, Entrepreneurship and Innovation" (NSRF 2014–2020) and co-financed by Greece and the European Union (European Regional Development Fund).

Declaration of interest: none.

The authors declare that they have no known competing financial interests or personal ~~relation~~ ~~ships~~relationships that could have appeared to influence the work reported in this paper.

CRediT authorship contribution statement

All authors contributed to the study conception and design. **Athanasia Panitsa**: Methodology, Validation, Investigation, original draft, Visualization. **Theano Petsi**: Methodology, Writing-review & editing. **Eleana Kordouli:** Methodology, Validation. **Poonam S. Nigam**: Result-analysis for writing-second draft, editing. **Maria Kanellaki**: Supervision. **Athanasios A. Koutinas**: Conceptualization, Writing-original draft, Project-administration, Funding-acquisition. All authors read and approved the final manuscript.

282

REFERENCES

1. Banvillet, G., Gatt, E., Belgacem, N., Bras, J., 2021. Cellulose fibers deconstruction by twin-screw extrusion with in situ enzymatic hydrolysis via bioextrusion. Bioresour. Technol. 327, 124819. https://doi.org/10.1016/j.biortech.2021.124819

2. Barouni, E., Petsi, T., Kanellaki, M., Bekatorou, A., Koutinas, A., 2015. Tubular cellulose/starch gel composite as food enzyme storehouse. Food Chem. 188, 106–110. https://doi.org/10.1016/j.foodchem.2015.04.038

3. Bian, H., Gao, Y., Yang, Y., Fang, G., Dai, H., 2018. Improving cellulose nanofibrillation of waste wheat straw using the combined methods of prewashing, p-toluenesulfonic acid hydrolysis, disk grinding, and endoglucanase post-treatment. Bioresour. Technol. 256, 321–327. https://doi.org/10.1016/j.biortech.2018.02.038

4. Cavali, M., Soccol, C.R., Tavares, D., Zevallos Torres, L.A., Oliveira de Andrade Tanobe, V., Zandoná Filho, A., Woiciechowski, A.L., 2020. Effect of sequential acid-alkaline treatment on physical and chemical characteristics of lignin and cellulose from pine (Pinus spp.) residual sawdust. Bioresour. Technol. 316, 123884. https://doi.org/10.1016/j.biortech.2020.123884

5. Chen, H., Mao, J., Jiang, B., Wu, W., Jin, Y., 2021. Carbonate-oxygen pretreatment of waste wheat straw for enhancing enzymatic saccharification. Process Biochem. 104, 117–123. https://doi.org/10.1016/j.procbio.2021.03.016

6. Chu, D., Deng, H., Zhang, X., Zhang, J., Bao, J., 2012. A simplified filter paper assay method of cellulase enzymes based on HPLC analysis. Appl. Biochem. Biotechnol. 167, 190–196. https://doi.org/10.1007/s12010-012-9673-0

7. Eatemadi, A., Daraee, H., Karimkhanloo, H., Kouhi, M., Zarghami, N., Akbarzadeh, A.,

306 Abasi, M., Hanifehpour, Y., Joo, S.W., 2014. Carbon nanotubes: Properties, synthesis,
307 purification, and medical applications. Nanoscale Res. Lett. 9,393.
308 https://doi.org/10.1186/1556-276X-9-393

309 8. FAO, 2019. Forest Products Annual Market Review, 2018-2019, Unece.

310 9. Gabriel, T., Belete, A., Syrowatka, F., Neubert, R.H.H., Gebre-Mariam, T., 2020.
311 Extraction and characterization of celluloses from various plant byproducts. Int. J. Biol.
312 Macromol. 158, 1248–1258. https://doi.org/10.1016/j.ijbiomac.2020.04.264

313 10. Ibrahim, K.S., 2013. Carbon nanotubes-properties and applications: a review. Carbon
314 Lett. 14, 131–144. https://doi.org/10.5714/cl.2013.14.3.131

315 11. Kargarzadeh, H., Ahmad, I., Abdullah, I., Dufresne, A., Zainudin, S.Y., Sheltami, R.M.,
316 2012. Effects of hydrolysis conditions on the morphology, crystallinity, and thermal stability
317 of cellulose nanocrystals extracted from kenaf bast fibers. Cellulose 19, 855–866.
318 https://doi.org/10.1007/s10570-012-9684-6

319 12. Koutinas, A., Papafotopoulou-Patrinou, E., Gialleli, A.I., Petsi, T., Bekatorou, A.,
320 Kanellaki, M., 2016a. Production of nanotubes in delignified porous cellulosic materials after
321 hydrolysis with cellulase. Bioresour. Technol. 213, 169–171.
322 https://doi.org/10.1016/j.biortech.2016.03.065

323 13. Koutinas, A., Papafotopoulou-Patrinou, E., Gialleli, A.I., Petsi, T., Bekatorou, A.,
324 Kanellaki, M., 2016b. Production of nanotubes in delignified porous cellulosic materials after
325 hydrolysis with cellulase. Bioresour. Technol. 213, 169–171.
326 https://doi.org/10.1016/j.biortech.2016.03.065

327 14. Krichen, F., Walha, S., Abdelmouleh, M., 2022. Hirshfeld surface analysis of the
328 intermolecular interaction networks in cellulose *Iα* and *Iβ*. Carbohydr. Res. 518, 108600.

https://doi.org/10.1016/j.carres.2022.108600

15. Kumar, A., Singh Negi, Y., Choudhary, V., Kant Bhardwaj, N., 2020. Characterization of Cellulose Nanocrystals Produced by Acid-Hydrolysis from Sugarcane Bagasse as Agro-Waste. J. Mater. Phys. Chem. 2, 1–8. https://doi.org/10.12691/jmpc-2-1-1

16. Li, C., Yang, Z., He Can Zhang, R., Zhang, D., Chen, S., Ma, L., 2013. Effect of pH on cellulase production and morphology of Trichoderma reesei and the application in cellulosic material hydrolysis. J. Biotechnol. 168, 470–477. https://doi.org/10.1016/j.jbiotec.2013.10.003

17. Lijima, S., 1991. Helical microtubules of graphitic carbon. Nature 354, 56-58. https://doi.org/10.1038/354056a0

18. Ling, Z., Tang, W., Su, Y., Shao, L., Wang, P., Ren, Y., Huang, C., 2021. Bioresource Technology Promoting enzymatic hydrolysis of aggregated bamboo crystalline cellulose by fast microwave-assisted dicarboxylic acid deep eutectic solvents pretreatments. Bioresour. Technol. 333, 125122. https://doi.org/10.1016/j.biortech.2021.125122

19. Nemmar, A., Vanbilloen, H., Hoylaerts, M.F., Hoet, P.H.M., Verbruggen, A., Nemery, B., 2001. Passage of Intratracheally Instilled Ultrafine Particles from the Lung into the Systemic Circulation in Hamster. Br. Commun. Am J Respir Crit Care Med 164, 1665–1668. https://doi.org/10.1164/rccm2101036

20. Panitsa, A., Petsi, T., Kandylis, P., Nigam, P.S., Kanellaki, M., Koutinas, A.A., 2021. Chemical preservative delivery in meat using edible vegetable tubular cellulose. LWT~~wt~~ 141, 111049. https://doi.org/10.1016/j.lwt.2021.111049

21. Park, S., Baker, J.O., Himmel, M.E., Parilla, P.A., Johnson, D.K., 2010. Cellulose crystallinity index: Measurement techniques and their impact on interpreting cellulase

performance. Biotechnol. Biofuels 3, 10. https://doi.org/10.1186/1754-6834-3-10

22. Poletto, M., Ornaghi Júnior, H.L., Zattera, A.J., 2014. Native cellulose: Structure, characterization and thermal properties. Materials (Basel). 7, 6105–6119. https://doi.org/10.3390/ma7096105

23. Reddy, J.P., Rhim, J.W., 2014. Characterization of bionanocomposite films prepared with agar and paper-mulberry pulp nanocellulose. Carbohydr. Polym. 110, 480–488. https://doi.org/10.1016/j.carbpol.2014.04.056

24. Satishkumar, B.C., Govindaraj, A., Nath, M., Rao, C.N.R., 2000. Synthesis of metal oxide nanorods using carbon nanotubes as templates. J. Mater. Chem. 10, 2115–2119. https://doi.org/10.1039/b002868l

25. Shankar, S., Rhim, J.W., 2016. Preparation of nanocellulose from micro-crystalline cellulose: The effect on the performance and properties of agar-based composite films. Carbohydr. Polym. 135, 18–26. https://doi.org/10.1016/j.carbpol.2015.08.082

26. Sosiati, H., Harsojo, H., 2014. Effect of combined treatment methods on the crystallinity and surface morphology of kenaf bast fibers. Cellul. Chem. Technol. 48 (1), 33–43.

27. Sosiati, H., Muhaimin, M., Purwanto, Wijayanti, D.A., Harsojo, Soekrisno, Triyana, K., 2015. Microscopic characterization of cellulose nanocrystals isolated from sisal fibers. Mater. Sci. Forum 827, 174–179. https://doi.org/10.4028/www.scientific.net/MSF.827.174

28. Sosiati, H., Muhaimin, M., Purwanto, Wijayanti, D.A., Triyana, K., 2014. Nanocrystalline Cellulose Studied with a Conventional SEM. 2014 Int. Conf. Physics, ICP 2014 12–15. https://doi.org/10.2991/icp-14.2014.3

29. USDA, 2021. World agricultural production. Ekon. APK.

374 30. Zhang, Q., Lu, Z., Su, C., Feng, Z., Wang, H., Yu, J., Su, W., 2021. High yielding, one-
375 step mechano-enzymatic hydrolysis of cellulose to cellulose nanocrystals without bulk
376 solvent. Bioresour. Technol. 331, 125015. https://doi.org/10.1016/j.biortech.2021.125015

377

Figure captions

Figure 1. XRD spectra of (a) untreated and (b) delignified freeze dried cellulosic materials.

Figure 2. FTIR spectra of untreated (black), delignified freeze dried (blue) and after hydrolysis (red) (a) corn cob and (b) sawdust, (c) FTIR spectra of solid formed by freeze dried samples of the supernatant after: 24 h (black), 72 h (blue), 168 h (red) and 336 h (pink) of corn cob's hydrolysis.

Figure 3. Porosimetry analysis of delignified cellulosic materials during their hydrolysis with cellulase. (a) BET surface area (m^2/g), (b) Pore volume (BJH) (cm^3/g), (c) Pore size (BET) (nm), (d) % pore volume between 2-70 nm of delignified freeze dried cellulosic materials during their hydrolysis with cellulase enzymes.

Figure 4. (a) TEM image of hydrolyzed corn cob (solid part) after 24 h of hydrolysis, (b) TEM image of solid formed by freeze-dried samples from supernatant after 72 h of corncob's hydrolysis.

Figure 5. Process flow sheet with mass (kg) and energy (kg of steam) balance for CHNTs production. 1. Delignification tank (100 m^3); 2. Enzyme production bioreactor (10 m^3); 3. Sterile filter (150 m^3/min); 4. Air pump (150 m^3/min); 5. CHNTs production bioreactor (100 m^3/min); 6. Pump (4 m^3/h); 7. Centrifugal separator (20 m^3/h); 8. Tank for CHNTs solution (100 m^3); 9. Condenser (3.3 m^3/h); 10. Freeze dryer – water removal (6000 kg/d); 11. Boiler (2500 kg oil/day); 12. Pump (20 m^3/h); 13. Vacuum pump 5Hp

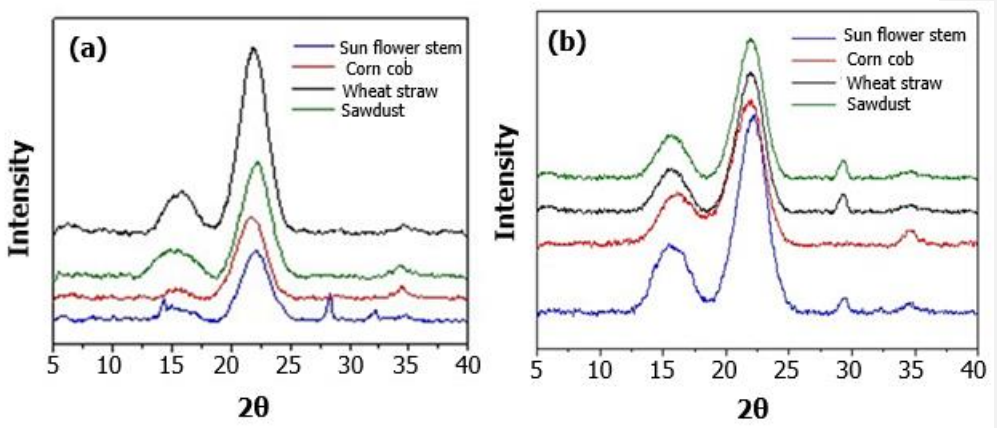

399
400 **Figure 1.**

401
402

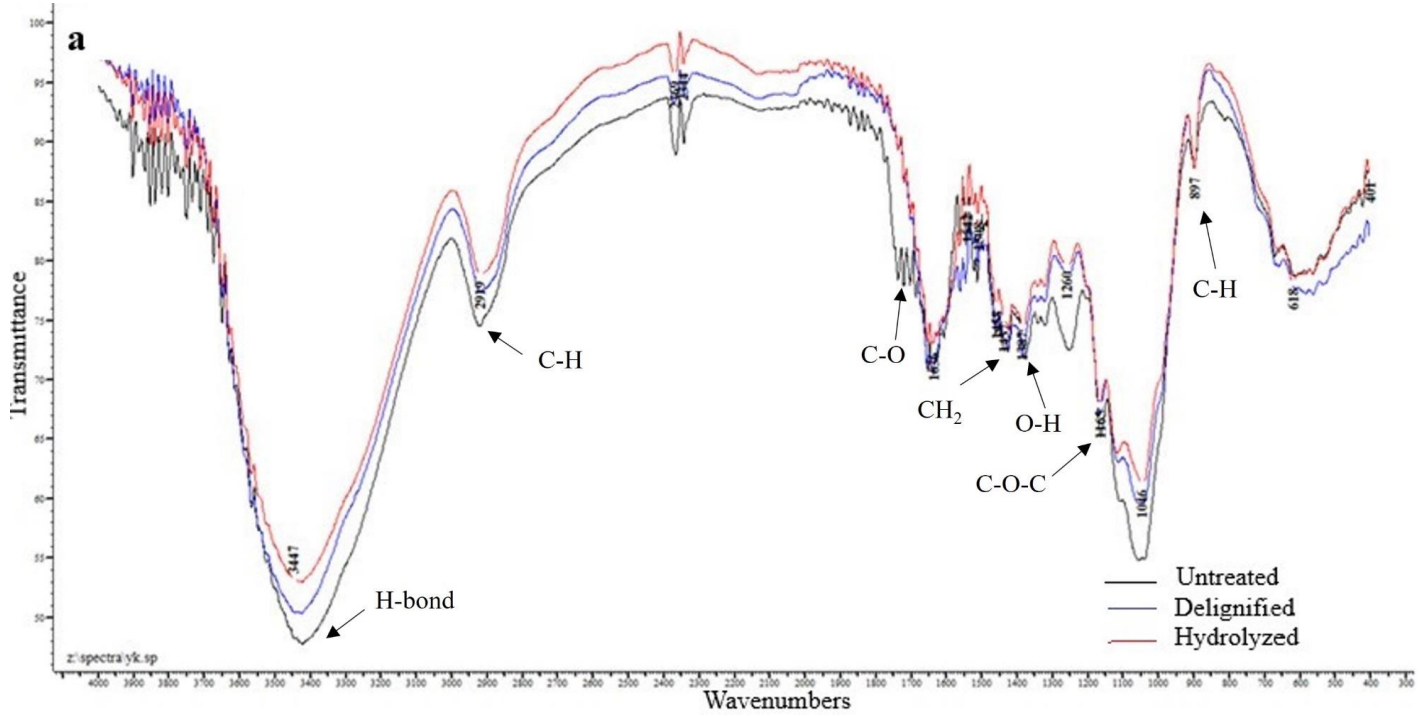

403
404 **Figure 2a.**

405

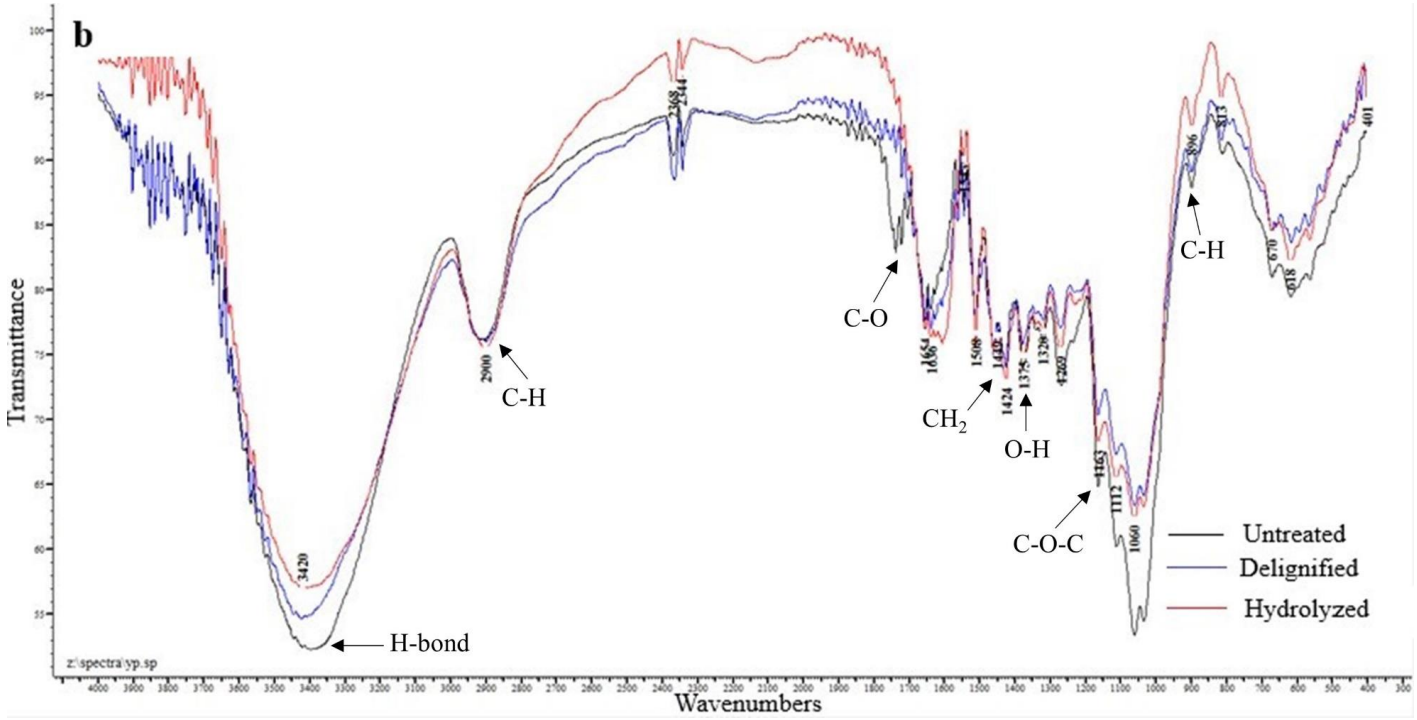

406

407

408 **Figure 2b.**

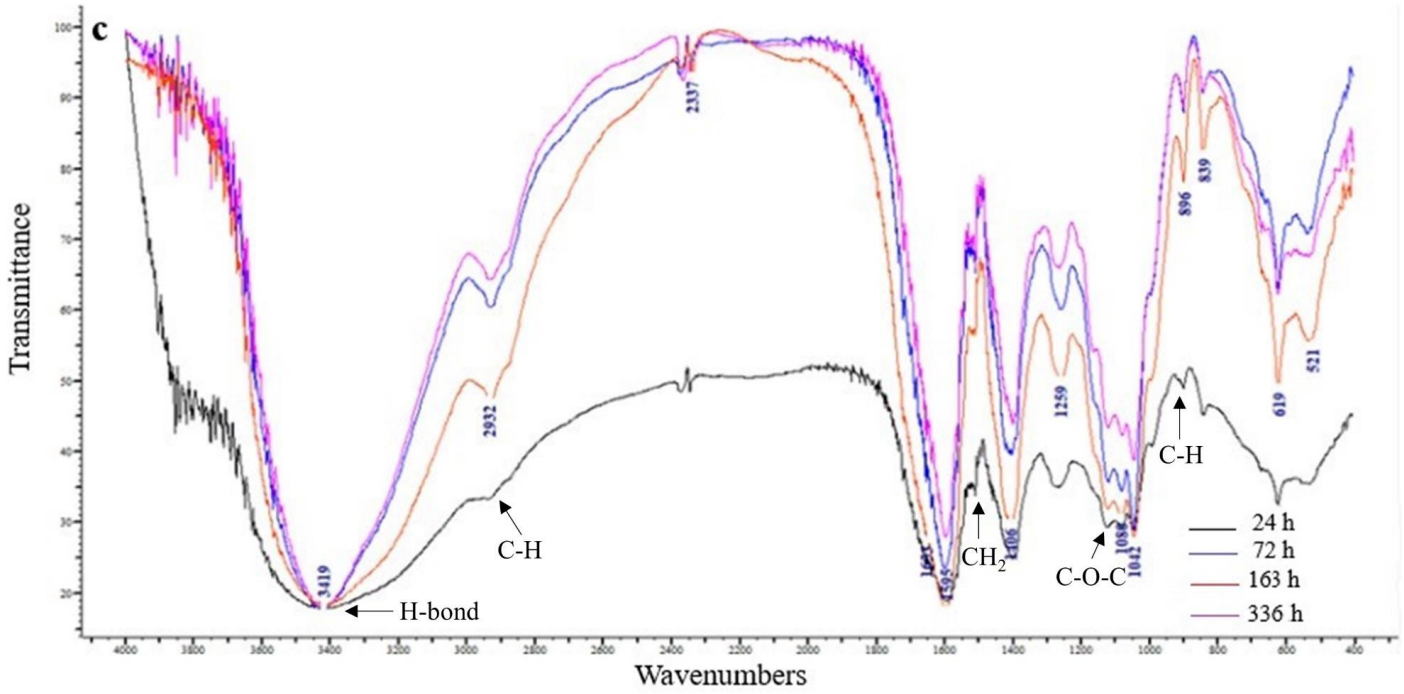
c
Transmittance
Wavenumbers
3419
2932
2337
1595
1259
1042
896
839
619
521
H-bond
C-H
CH2
C-O-C
C-H
24 h
72 h
163 h
336 h

Figure 2c.

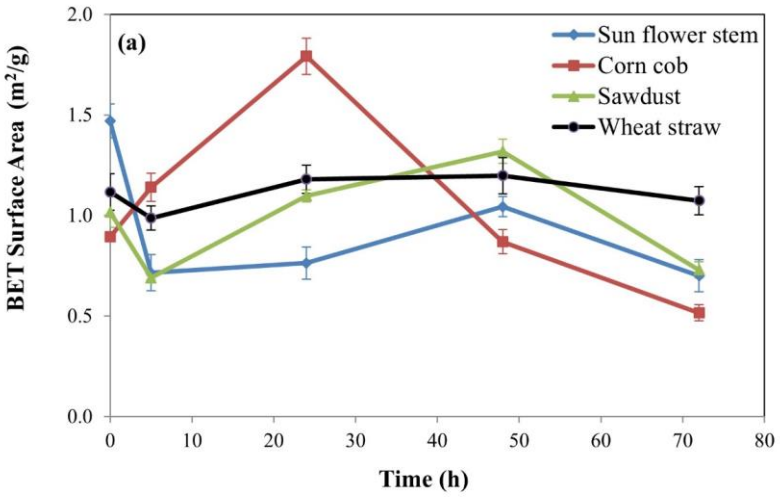
(a)
BET Surface Area (m²/g)
Time (h)
Sun flower stem
Corn cob
Sawdust
Wheat straw
2.0
1.5
1.0
0.5
0.0
0
10
20
30
40
50
60
70
80

Figure 3a.

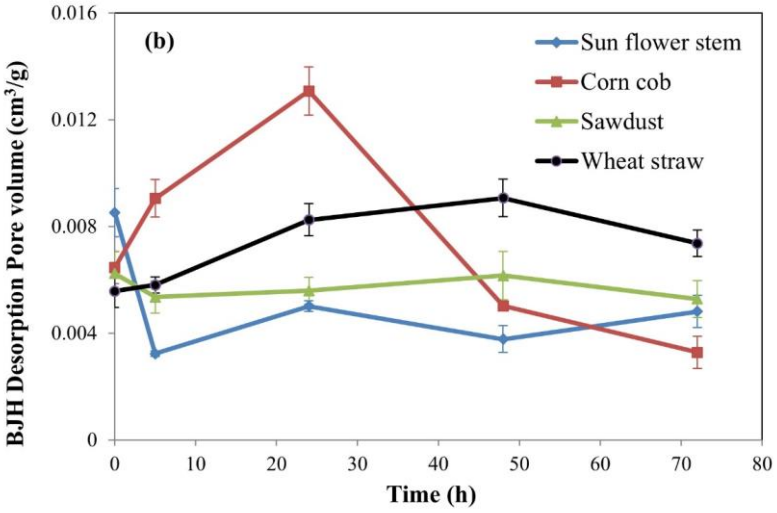
(b)
Sun flower stem
Corn cob
Sawdust
Wheat straw
BJH Desorption Pore volume (cm3/g)
0.016
0.012
0.008
0.004
0
0
10
20
30
40
50
60
70
80
Time (h)

Figure 3b.

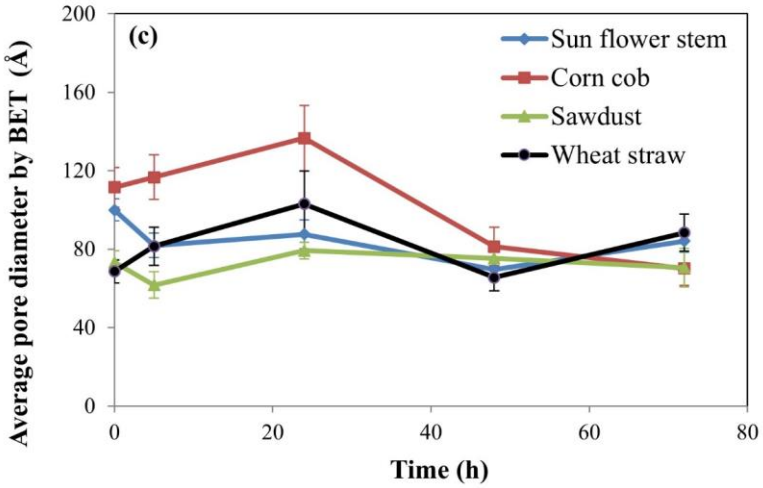
(c)
Sun flower stem
Corn cob
Sawdust
Wheat straw
Average pore diameter by BET (Å)
Time (h)
200
160
120
80
40
0
0
20
40
60
80

Figure 3c.

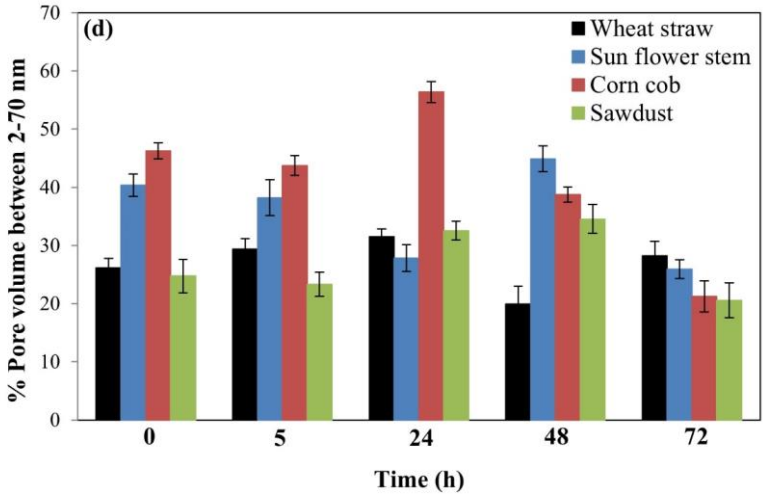
(d)
Wheat straw
Sun flower stem
Corn cob
Sawdust
% Pore volume between 2-70 nm
70
60
50
40
30
20
10
0
0
5
24
48
72
Time (h)

Figure 3d.

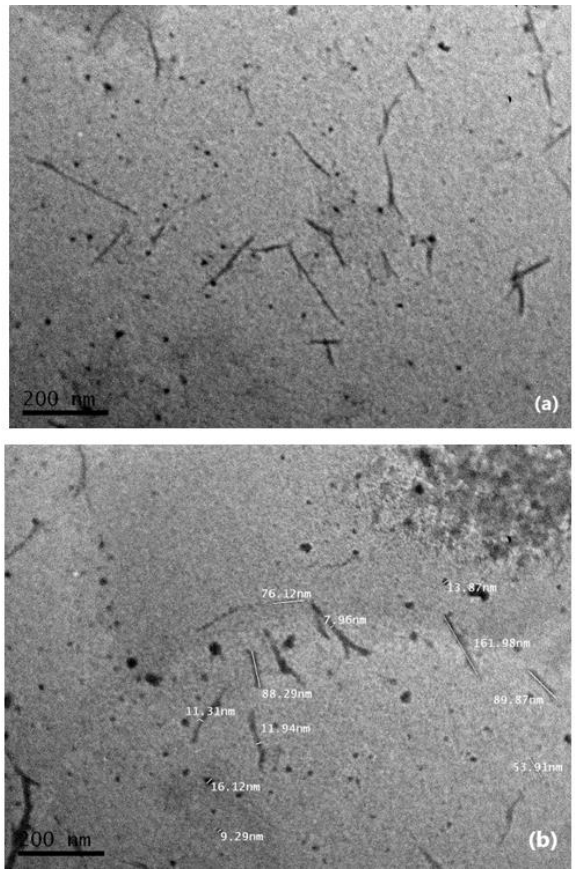
200 nm
(a)
76.12nm
13.87nm
7.96nm
161.98nm
88.29nm
89.87nm
11.31nm
11.94nm
53.91nm
16.12nm
200 nm
9.29nm
(b)

Figure 4.

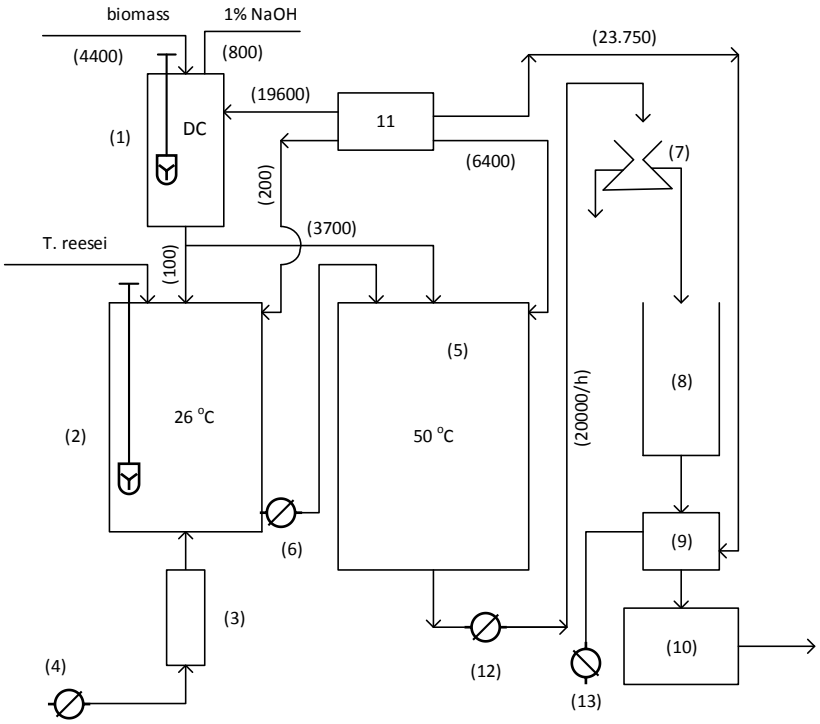
biomass
1% NaOH
(4400)
(800)
(19600)
(1)
DC
11
(23.750)
(6400)
(7)
(200)
(3700)
T. reesei
(100)
(5)
(8)
(2)
26 °C
50 °C
(20000/h)
(6)
(9)
(3)
(10)
(4)
(12)
(13)

Figure 5.

493 **Table 1.** Porosimetry analysis of untreated and delignified freeze dried (TC) cellulosic materi-
494 als.
495

	BET Surface area (m^2/g)		**Pore volume$_{(BJH)}$ (cm^3/g)**		**Pore size$_{(BET)}$ (nm)**	
Cellulosics	Untreated	TC	Untreated	TC	Untreated	TC
Wheat straw	0.48 ± 0.01	1.12 ± 0.09	0.0034 ± 0.0006	0.0056 ± 0.0006	8.23 ±0. 95	6.85± 0.8
Sun flower stem	1.70 ± 0.08	1.47 ± 0.09	0.0060 ± 0.0008	0.0085 ± 0.0009	6.41 ± 0.97	9.99 ± 1.00
Corn cob	0.34 ± 0.02	0.89 ± 0.01	0.0026 ± 0.0004	0.0065 ± 0.0006	8.78 ± 0.82	11.14 ± 1.32
Sawdust	0.60 ± 0.02	1.02 ± 0.08	0.0033 ± 0.0007	0.0062 ± 0.0008	4.48 ± 0.64	7.33 ± 0.89

496 **Table 2.** Crystallinity degree and crystallite size of untreated, delignified (TC) and hydro-
497 lyzed freeze dried cellulosic materials.

Cellulosics	**Percentage of crystallinity (%)**			**Crystal size (nm)**		
	Untreated	TC	Hydrolyzed	Untreated	TC	Hydrolyzed
Wheat straw	53.0	61.6	66.5	31.7	3.3	3.9
Sunflower stem	66.2	57.7	61.9	31.2	3.0	3.8
Corn cob	45.3	58.0	61.6	30.7	3.1	3.6
Sawdust	56.6	60.8	59.5	30.4	3.3	3.5

498

499 **Table 3.** Porosimetry analysis of freeze dried samples from supernatant during corn cob's hy-
500 drolysis with cellulase.

501

	BET Surface area (m^2/g)	**Pore volume$_{(BJH)}$ (cm^3/g)**	**Pore size$_{(BET)}$ (nm)**
24 h	0.79±0.03	0.0040±0.0001	3.60 ± 0.2
72 h	1.35±0.1	0.0069±0.0005	4.60 ± 0.6
168 h	0.20±0.009	0.0011±0.0003	1.65 ± 0.3
336 h	0.35±0.04	0.0025±0.0002	1.60 ± 0.3

502

503 **Table 4.** Investment cost. Equipment cost for plant installation.

Machinery	Capacity	Price (€)
Delignification tank	100,000 L	30,000
Enzyme production bioreactor	10,000 L	20,000
Sterile filter	150 m^3/min	9,000
Air pump	150 m^3/min	20,000
CHNTs production bioreactor	100,000 L	30,000
Pump	4 m^3/h	2,000
Centrifugal separator	20 m^3/h	150,000
Tank for CHNTs solution	100,000 L	30,000
Condenser	3.3 m^3/h	300,000
Freeze dryer	6000 Kg water/day	500,000
Boiler	2500 Kg oil/day	600,000
Pump	20 m^3/h	2,000
Vacuum pump	5 HP	20,000
Pipe lines		30,000
Total		1,743,000

504 **Table 5.** Daily Production Cost. Parameters affecting the production cost.

505

Parameter	Cost (€/day)
Raw material	400
Labor cost	1,070
Thermal energy	830
Electricity	35
Water requirement	40
Consumables	205
Investment payments	156
Total	2731

Figure

Click here to access/download;Figure;FIGURE 1.docx

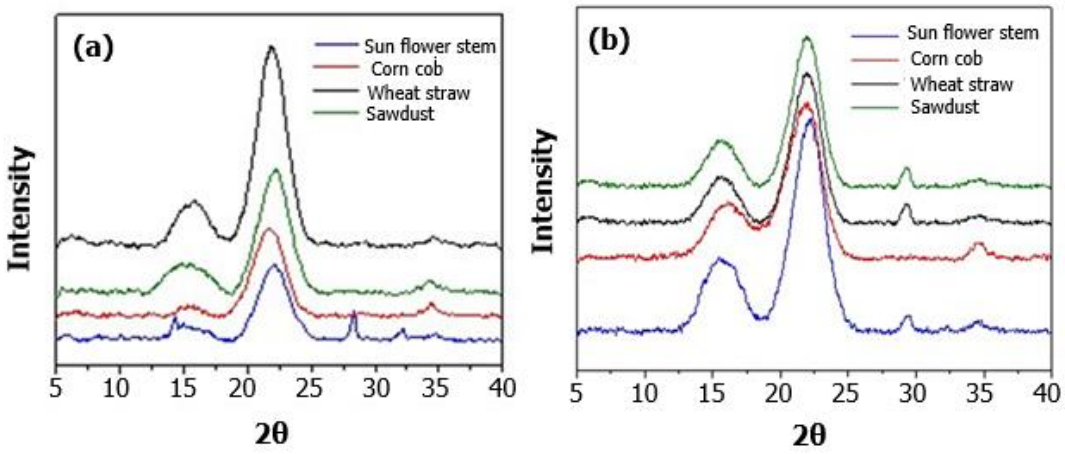

Figure

Click here to access/download;Figure;Figure 2.docx

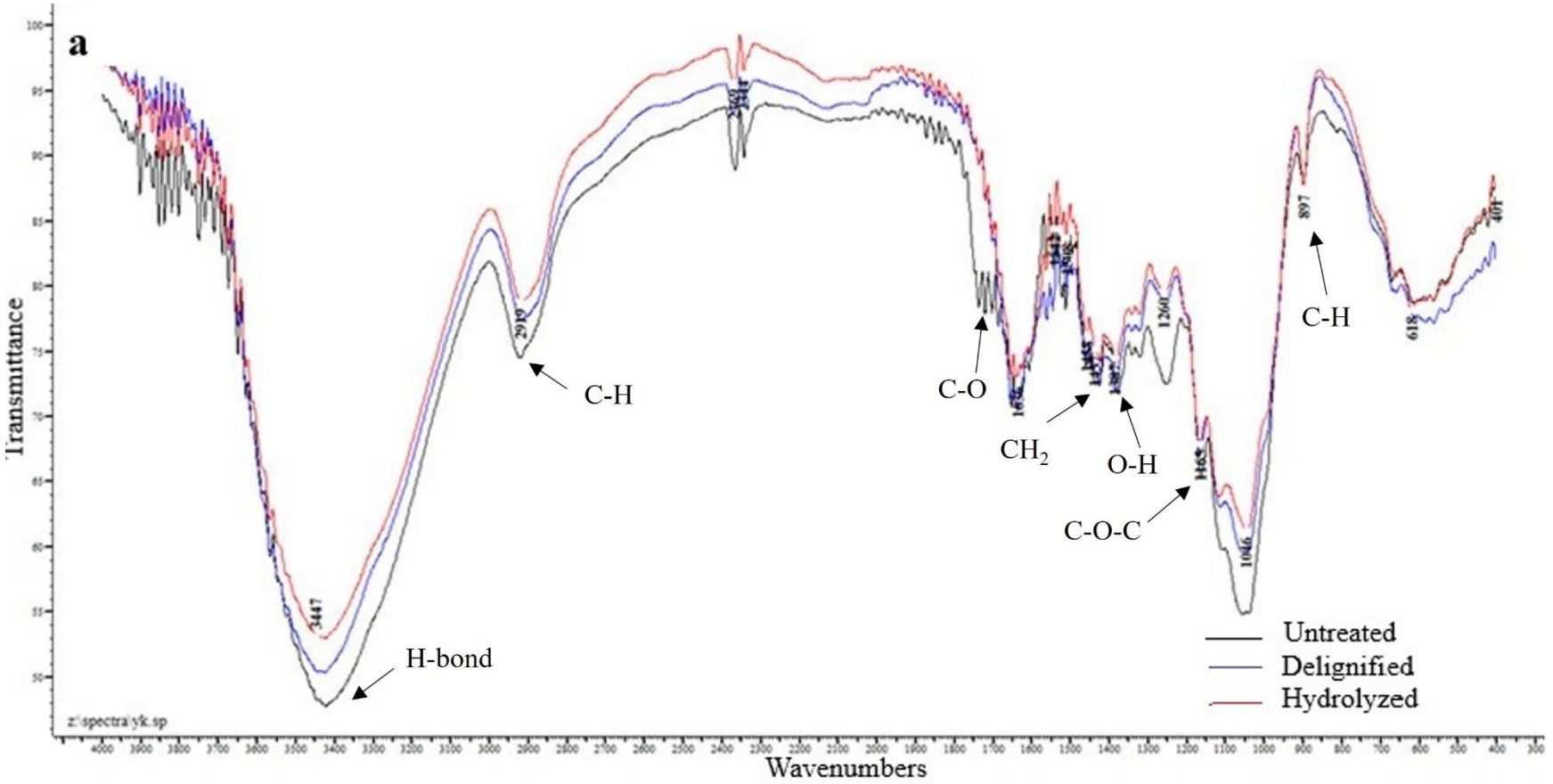

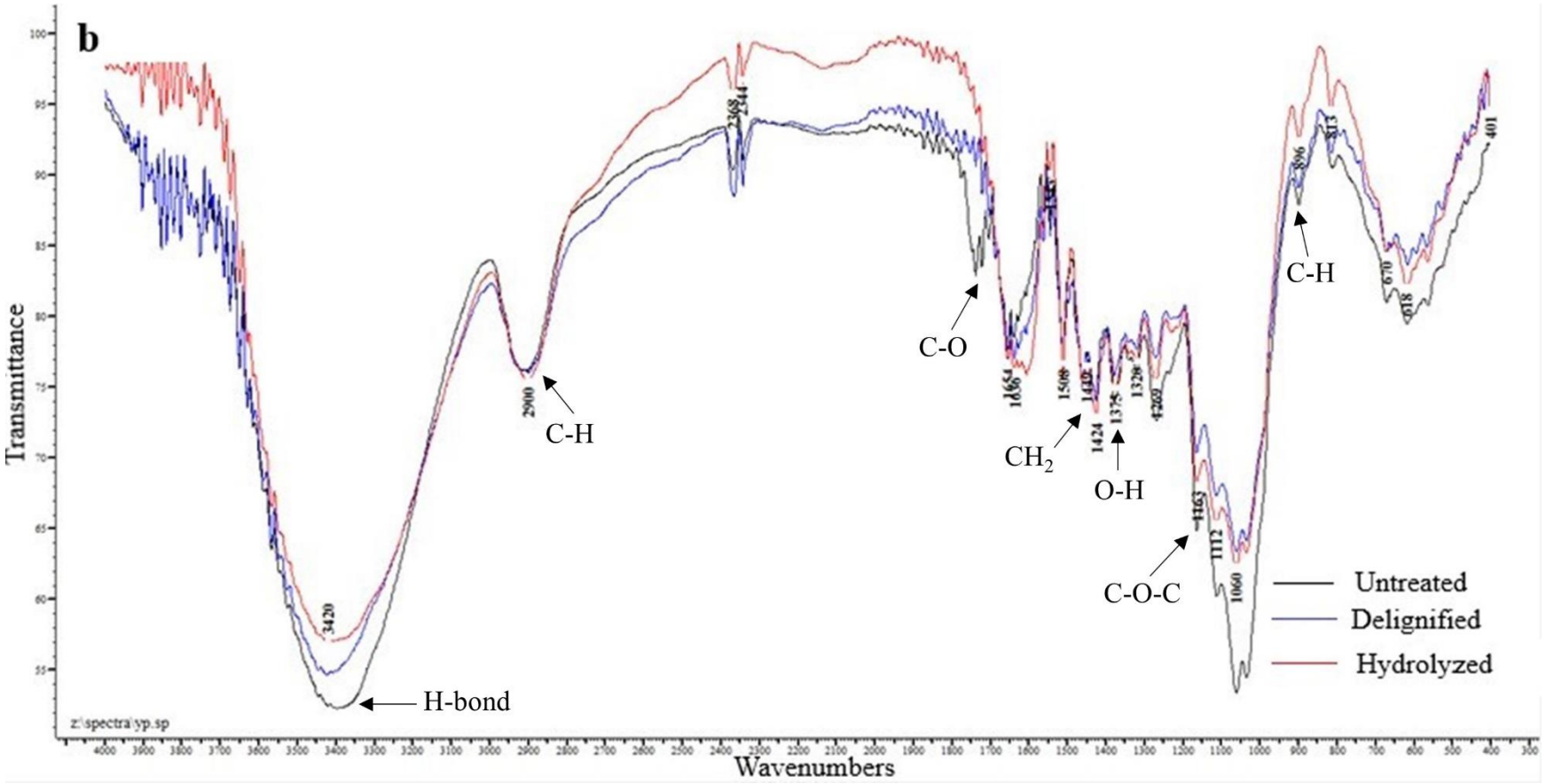
b
Transmittance
Wavenumbers
H-bond
C-H
C-O
CH2
O-H
C-O-C
C-H
Untreated
Delignified
Hydrolyzed
z:\spectra\yp.sp

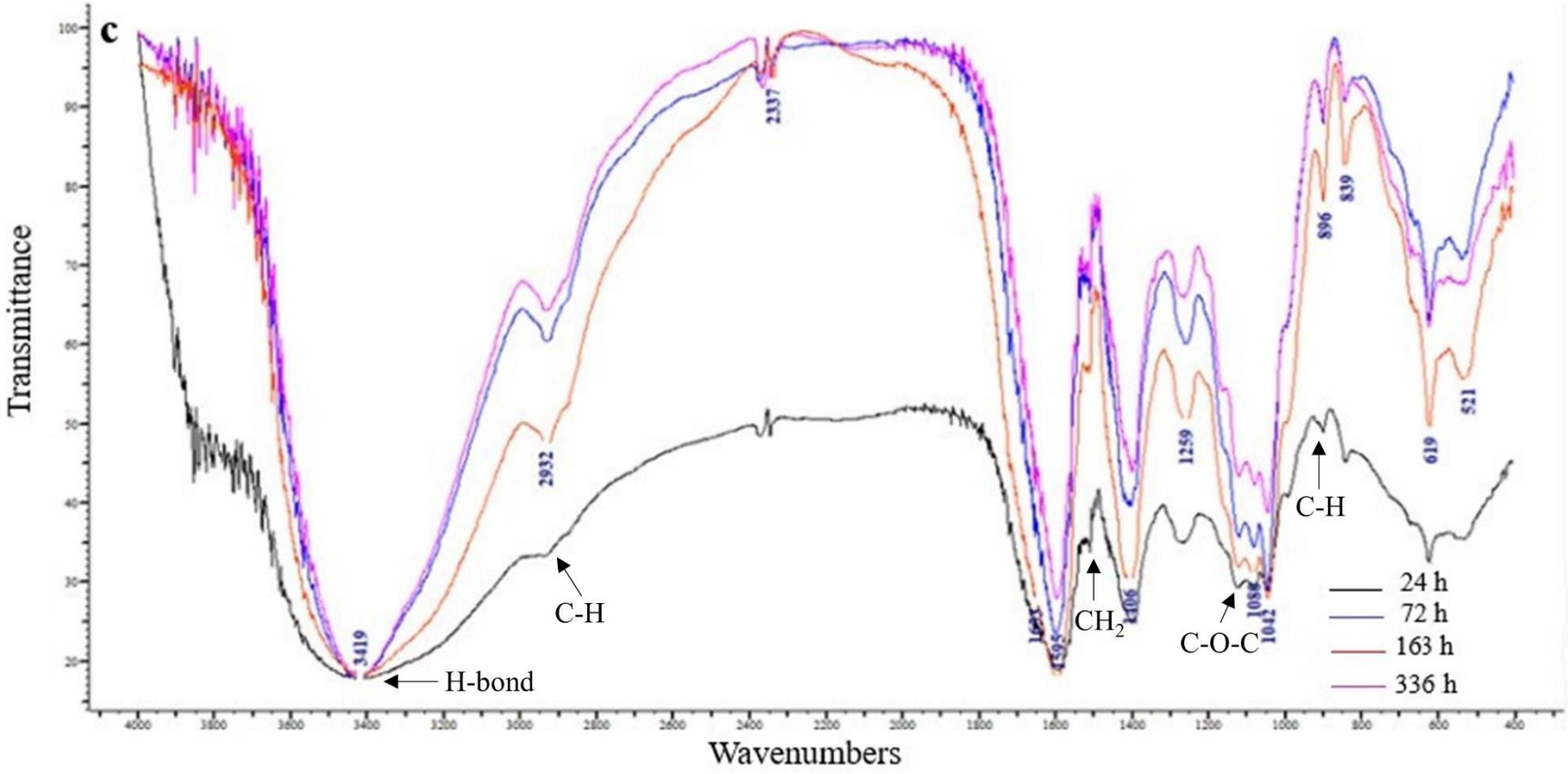
c
Transmittance
Wavenumbers
3419
2932
2337
1595
1259
1042
896
839
619
521
H-bond
C-H
CH2
C-O-C
C-H
24 h
72 h
163 h
336 h

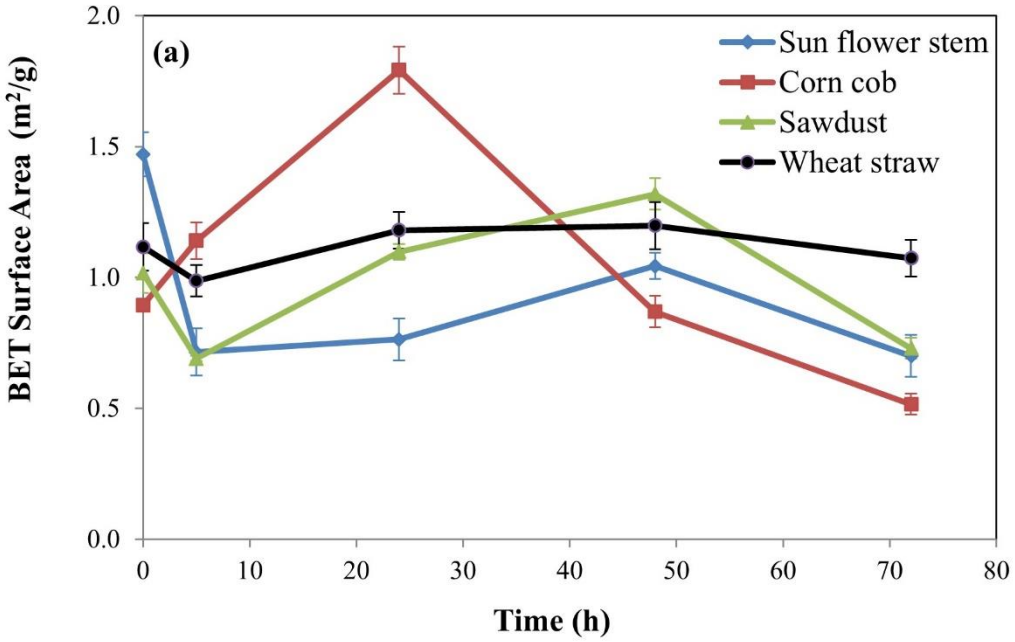

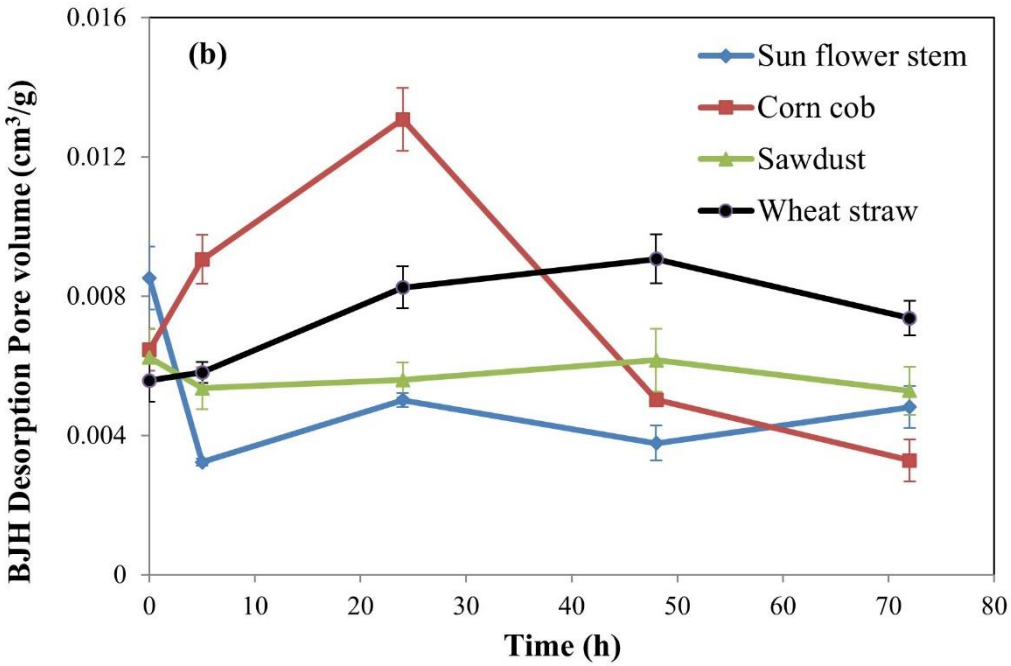

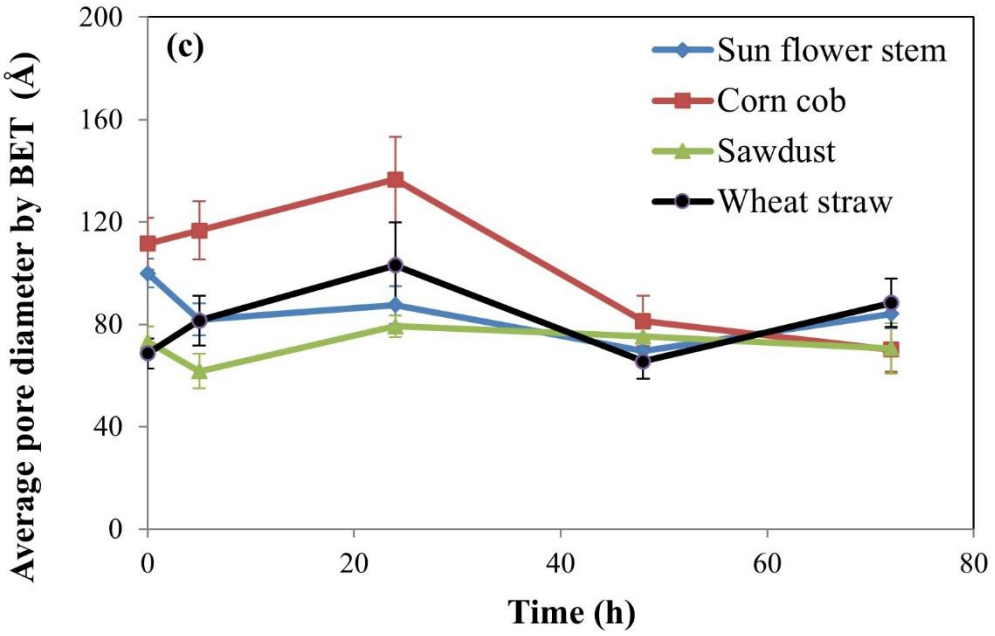
(c)
Sun flower stem
Corn cob
Sawdust
Wheat straw
Average pore diameter by BET (Å)
200
160
120
80
40
0
0
20
40
60
80
Time (h)

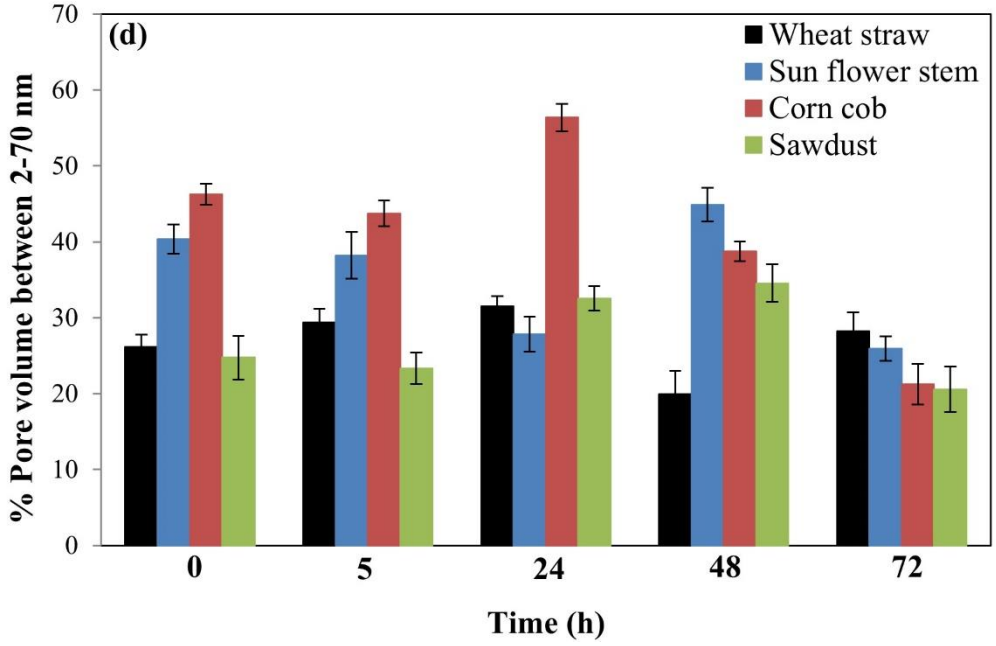
(d)
Wheat straw
Sun flower stem
Corn cob
Sawdust
% Pore volume between 2-70 nm
70
60
50
40
30
20
10
0
0
5
24
48
72
Time (h)

Figure

Click here to access/download;Figure;FIGURE 4.docx

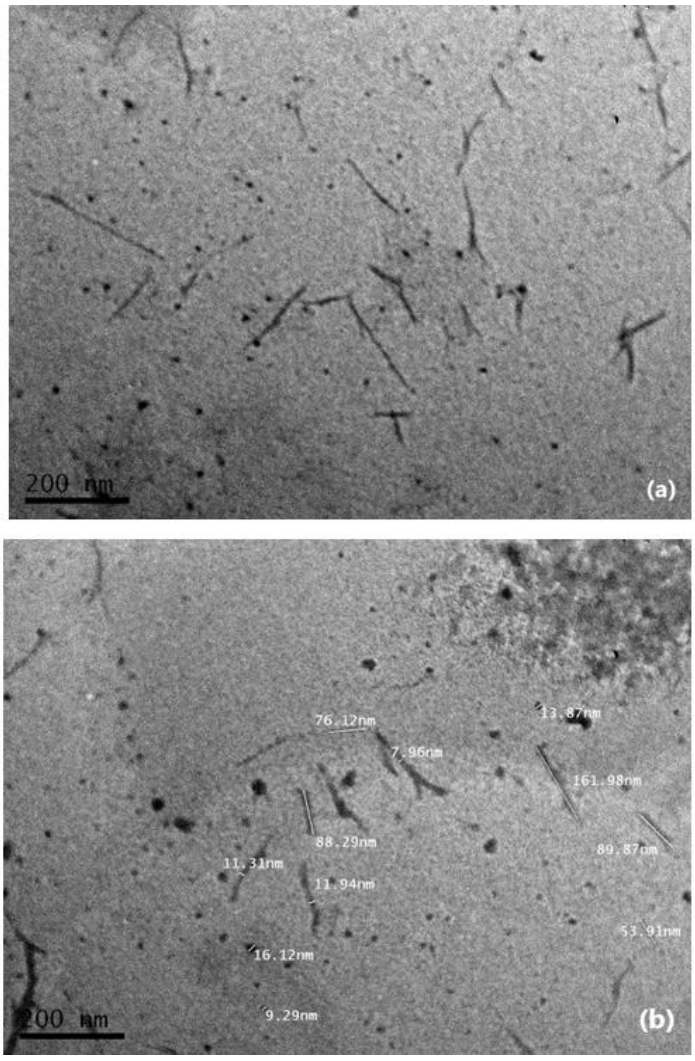

Figure

Click here to access/download;Figure;FIGURE 5.docx

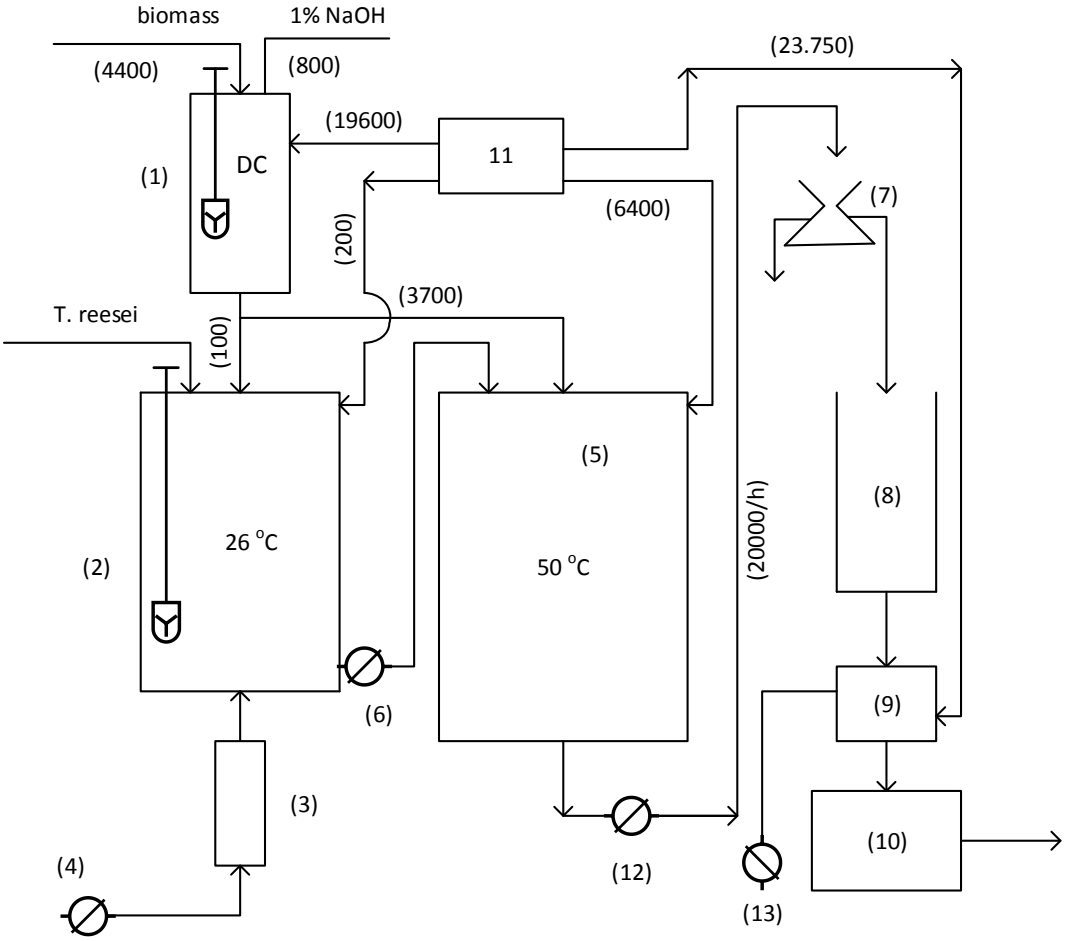

	BET Surface area (m^2/g)		Pore volume$_{(BJH)}$ (cm^3/g)		Pore size$_{(BET)}$ (nm)	
Cellulosics	Untreated	TC	Untreated	TC	Untreated	TC
Wheat straw	0.48 ± 0.01	1.12 ± 0.09	0.0034 ± 0.0006	0.0056 ± 0.0006	8.23 ±0. 95	6.85± 0.8
Sun flower stem	1.70 ± 0.08	1.47 ± 0.09	0.0060 ± 0.0008	0.0085 ± 0.0009	6.41 ± 0.97	9.99 ± 1.00
Corn cob	0.34 ± 0.02	0.89 ± 0.01	0.0026 ± 0.0004	0.0065 ± 0.0006	8.78 ± 0.82	11.14 ± 1.32
Sawdust	0.60 ± 0.02	1.02 ± 0.08	0.0033 ± 0.0007	0.0062 ± 0.0008	4.48 ± 0.64	7.33 ± 0.89

Cellulosics	Percentage of crystallinity (%)			Crystal size (nm)		
	Untreated	TC	Hydrolyzed	Untreated	TC	Hydrolyzed
Wheat straw	53.0	61.6	66.5	31.7	3.3	3.9
Sunflower stem	66.2	57.7	61.9	31.2	3.0	3.8
Corn cob	45.3	58.0	61.6	30.7	3.1	3.6
Sawdust	56.6	60.8	59.5	30.4	3.3	3.5

	BET Surface area (m^2/g)	Pore volume$_{(BJH)}$ (cm^3/g)	Pore size$_{(BET)}$ (nm)
24 h	0.79±0.03	0.0040±0.0001	3.60 ± 0.2
72 h	1.35±0.1	0.0069±0.0005	4.60 ± 0.6
168 h	0.20±0.009	0.0011±0.0003	1.65 ± 0.3
336 h	0.35±0.04	0.0025±0.0002	1.60 ± 0.3

Machinery	Capacity	Price (€)
Delignification tank	100,000 L	30,000
Enzyme production bioreactor	10,000 L	20,000
Sterile filter	150 m^3/min	9,000
Air pump	150 m^3/min	20,000
CHNTs production bioreactor	100,000 L	30,000
Pump	4 m^3/h	2,000
Centrifugal separator	20 m^3/h	150,000
Tank for CHNTs solution	100,000 L	30,000
Condenser	3.3 m^3/h	300,000
Freeze dryer	6000 Kg water/day	500,000
Boiler	2500 Kg oil/day	600,000
Pump	20 m^3/h	2,000
Vacuum pump	5 HP	20,000
Pipe lines		30,000
Total		1,743,000

Parameter	Cost (€/day)
Raw material	400
Labor cost	1,070
Thermal energy	830
Electricity	35
Water requirement	40
Consumables	205
Investment payments	156
Total	2731

Declaration of interests

☒The authors declare that they have no known competing financial interests or personal relationships that could have appeared to influence the work reported in this paper.

☐The authors declare the following financial interests/personal relationships which may be considered as potential competing interests:

CRediT authorship contribution statement

Athanasia Panitsa: Methodology, Validation, Investigation, Writing - original draft, Visualization. **Theano Petsi**: Methodology, Writing - review & editing. **Eleana Kordouli:** Methodology, Validation. **Poonam S. Nigam**: Result-analysis for writing-second draft, editing. **Maria Kanellaki**: Supervision. **Athanasios A. Koutinas**: Conceptualization, Writing - original draft, Project administration, Funding acquisition.